Geoarchaeology

WILEY

Geoarchaeology An International Journal

RESEARCH ARTICLE OPEN ACCESS

Fire Use During the Last Glacial Maximum: Evidence From the Epigravettian at Korman' 9, Middle Dniester Valley, Ukraine

William Chase Murphree[1] | Cruz Ferro-Vázquez[2] | Larissa Kulakovska[3] | Vitalii I. Usyk[3,4] | Olesia Kononenko[3] | Marjolein D. Bosch[5,6,7,8] | Paul Haesaerts[9] | Freddy Damblon[9] | Stéphane Pirson[10,11] | Philip R. Nigst[7,8] | Vera Aldeias[1]

[1]Interdisciplinary Center for Archaeology and the Evolution of Human Behaviour (ICArEHB), Universidade do Algarve, Faro, Portugal | [2]INCIPIT-CSIC, Cidade da Cultura, Edificio Fontán, Santiago de Compostela, Spain | [3]Institute of Archaeology, National Academy of Sciences of Ukraine, Kyiv, Ukraine | [4]Institute of Archaeology, Czech Academy of Sciences, Brno, Czechia | [5]Research Group Prehistoric Identities, Department of Prehistory and Western Asia and North African Archaeology, Austrian Archaeological Institute, Austrian Academy of Sciences, Vienna, Austria | [6]Department of Prehistory, Natural History Museum, Vienna, Austria | [7]Department of Prehistoric and Historical Archaeology, University of Vienna, Vienna, Austria | [8]Human Evolution and Archaeological Sciences (HEAS), University of Vienna, Vienna, Austria | [9]Royal Belgian Institute of Natural Science, Brussels, Belgium | [10]Agence wallonne du Patrimoine (AWaP), Service Public de Wallonie, Direction d'appui scientifique et technique, Jambes, Belgium | [11]Department of Geology, European Archaeometry Centre, University of Liège, Liège, Belgium

Correspondence: William Chase Murphree (wmurphree@ualg.pt)

Received: 20 February 2025 | **Revised:** 20 February 2025 | **Accepted:** 3 March 2025

Scientific Editor: Mentzer Susan M

Keywords: colorimetric analysis | fire use | LGM | micromorphology | Upper Palaeolithic

ABSTRACT

The Last Glacial maximum (LGM), spanning from 26.5 to 19 thousand years before present (ka BP), is a period of extreme climatic degradation associated with reduced biomass production and resource stress throughout Eurasia. Arguably, one of the most fundamental tools for human survival during this cold and arid period was the ability to create, maintain and use fire. While fire is widely considered a ubiquitous tool in modern human behaviour, there are surprisingly few well-described combustion features during the LGM in Europe. In this paper, we provide high-resolution geoarchaeological research into three combustion features associated with Epigravettian occupations at the site of Korman' 9 (Ukraine) with ages falling in the LGM. Our results show distinct variations in the size and structure of the combustion features, potentially indicating multiple occupations within the same layer or reflect differences in site organization or function during a single occupation. Additionally, our analysis shows clear evidence of the effect of solifluction and the lack of preservation of the ash layer(s) of the combustion features, as well as the development of bioturbation features enhanced by anthropogenic input. To better estimate heating temperatures of the combustion events, we employed a novel approach using colour analysis showing temperatures reaching 600°C in the substrate underlying the combustion features. In all, the combustion features at Korman' 9 provide invaluable new insights as well as high resolution description of pyrotechnological behaviours during the LGM, which has been lacking during this critical period in our evolutionary history.

Philip R. Nigst and Vera Aldeias are co-last authors.

1 | Introduction

The Last Glacial Maximum (LGM) in Europe, roughly 26.5 through 19 thousand years before present (ka BP), corresponds to the latest period where the global volume of ice reached it maximum extent within the northern hemisphere (e.g., Hughes and Gibbard 2015; (Mix 2001). This period is characterized by rapid climatic deterioration, with extreme cold and arid conditions resulting in habitat loss and geographic isolation (e.g., Banks et al. 2008). These harsh climatic conditions are thought to have greatly impacted the distribution of Upper Palaeolithic anatomically modern human (AMH) populations and influenced both their behaviour and technology (Banks et al. 2008; Moreau et al. 2021). It's commonly hypothesized that populations were geographically isolated in so-called refugia in the Balkans (Stiner et al. 2022) or Western Europe, including southern France and Iberia, where conditions were more favourable for both humans and animals (Straus 2015). Whereas areas like the Middle Danube region of Central Europe show a clear decrease in population densities, with prevalence of spatially smaller and more widely scattered sites (Škrdla et al. 2021, 164). Moreover, from a lithic technological aspect, there is a clear trend for more regionalized named stone tool industries, such as the Solutrean in southwestern Europe and the Epigravettian in central, southern, southeastern and eastern Europe (e.g., Banks et al. 2008; Hauck et al. 2017; Kulakovska et al. 2021; Nuzhnyi 2006; Straus 2015).

The LGM landscape in eastern Europe can be generally characterized by open and boreal steppe environments with numerous river systems flowing into the Black and Caspian Seas (Demidenko 2021; Maier et al. 2023; Willis & Van Andel 2004). The East European Plain is constrained by the Urals to the east and the Carpathian Mountains to the southwest. Many of the sites occupied during the LGM are located near the banks of the major river systems, with a significant number of known sites located on the Don (Russia), Prut (Romania and Ukraine), Dnieper and Dniester rivers in Ukraine and Moldova (Klein 1973; Nigst et al. 2021; Noiret 2009; Noiret et al. 2021; Noiret and Otte 2010). Similarly, to central Europe, Epigravettian occupations during the LGM appear to be ephemeral in nature with lower density of finds compared to the earlier Gravettian technocomplex (Anghelinu et al. 2020; Demay et al. 2021; Demidenko 2021; Škrdla et al. 2021).

It is widely assumed that a key tool for human survival, particularly during cold periods, is the ability to create, maintain and use fire (Gilligan 2010; Gowlett 2006; Roebroeks and Villa 2011; Sandgathe et al. 2011). A large body of literature has provided data on the benefits of fire use on hominin evolution and its fundamental function in everyday life (Aiello and Wheeler 1995; Mallol and Henry 2017; Roebroeks and Villa 2011; Stahlschmidt et al. 2020; Wrangham 2017). More recent papers on experimental and ethnographic research have also shown the labour-intensive nature of using pyrotechnology; meaning fire use is not only an essential survival tool but also played a key role in how hunter-gatherer populations organize themselves (Mallol and Henry 2017; McCauley et al. 2020; Pryor et al. 2016). This includes: how hunter-gatherers acquire resources like wooden fuels (Beresford-Jones et al. 2010; Pryor et al. 2016), if they stored or cached fuel materials for future use (Beresford-Jones et al. 2011; Pryor et al. 2016), how they started and maintained fires (Mallol and Henry 2017; Mallol et al. 2007; McCauley et al. 2020), or how sites and activities are organized around combustion features (Clark et al. 2022; Galanidou 1997; Rolland 2004, 2018).

While there are several on-going debates on the prevalence of habitual fire use behaviour in early hominins (Roebroeks and Villa 2011; Sandgathe 2017; Sandgathe et al. 2011; Stahlschmidt et al. 2015) or even in later European Middle Palaeolithic (Dibble et al. 2017; Dibble et al. 2018; Sorensen et al. 2014; Sorensen 2017), it's widely assumed that pyrotechnology was a ubiquitous behavioural adaptation during the Upper Palaeolithic (Chazan 2017; Pryor et al. 2016). It is, therefore, surprising that in a recent review (Murphree and Aldeias 2022)—authored by some of us—on the available data on Upper Palaeolithic found an overall lack of well- described combustion features during the LGM. We currently lack both macro- and micromorphological descriptions of fire features for this period beyond brief mentions of presence of features or combustion-related residues (such as concentrations of charcoal, ash or indirect proxies of fire use like burned lithics). This scarcity of published data could be attributed to several factors, namely: either lack of preservation of fire remains during cold periods, a publication bias, or a potential lack of widespread fire use by modern humans during this period (Murphree and Aldeias 2022). Concerning the latter possibility, we could consider that, with the onset of extreme cold conditions, the lack of available wood fuel in steppe and grassland environments could have been an issue in which case human groups used other behavioural adaptions to survive, namely the consumption of rotten meat (Speth 2017).

To address a possible gap of publications and preservation bias, we must better understand how we recognize and describe fire use in the archaeological record, both in the field and in subsequent reporting. Upper Palaeolithic combustion features vary significantly in terms of their structure: ranging from open flat hearths to potential kiln-like structures found at Upper Palaeolithic sites in Moravia (Mallol et al. 2017; Murphree and Aldeias 2022; Svoboda et al. 2018). Based on the available descriptions of combustion features, it can be suggested that open flat hearths dominate the LGM and post-LGM landscape of Europe (Murphree and Aldeias 2022). These simple flat combustion features are commonly comprised of three distinct strata: a reddish-brown basal layer, followed by a black, organic-rich layer overlain by a white/grey layer (Aldeias et al. 2016; Goldberg et al. 2017; Mallol et al. 2013b; Mallol et al. 2017; Mentzer 2014). A basal rubified layer can result from the thermal alteration of a substrate on top of which a hearth was built (Aldeias et al. 2016; Canti and Linford 2000; Ferro-Vázquez et al. 2021; March et al. 2014). While the presence of a black layer consists of burned material related to either the occupational surface on which the fire was built or fuel that was not fully combusted (Mallol et al. 2013a; Mallol et al. 2013b). In well-preserved features, the uppermost whitish layer is typically rich in ash and is the result of the complete combustion of wooden fuels (Braadbaart et al. 2012; Canti 2003; Karkanas 2021; Karkanas et al. 2002). These distinctions are important as much sedimentary features, like combustion features, are susceptible to syn- and post-depositional alterations.

Combustion remains can easily be displaced by human actions (such as trampling or hearth rake out), whereas ashes can be dissolved or blown away by wind if left in an exposed surface (Goldberg et al. 2017; Miller et al. 2010; Schiegl et al. 2003). As a result, the identification of fire features based solely on field observations is not always straightforward, which may have an implication on the lack of in-depth archaeological reporting of so-called simple flat combustion features. Moreover, as fire can be either natural or anthropogenic in origin, the distinction between the two can, at times, be problematic (Goldberg et al. 2017; Mentzer 2014; Stahlschmidt et al. 2015). Generally, there is a clear need to better standardize the descriptions and consistently report combustion features in archaeology.

In this paper, we present both macroscopic field-based descriptions and microstratigraphic analysis of three combustion features associated with Epigravettian occupations of Korman′ 9, Ukraine. The combustion features were located in two separate archaeological layers (AL I and AL II) dating to around the height of the LGM, approx. 23–21 ka BP (Kulakovska et al. 2021). Macro-stratigraphic descriptions are based on the criteria outlined by Mallol et al. (2017) and Murphree and Aldeias (2022), while higher resolution analysis was conducted through employing soil micromorphological techniques, with descriptions following the nomenclature of Stoops (2003). We also provide a colorimetric analysis of the red layers for firing temperature estimation as proposed by Ferro-Vázquez et al. (2021). We then compare the results of our study in terms of similarities with neighbouring LGM sites. Finally, we discuss our results for understanding how combustion features and residues are preserved in periglacial conditions and their implications for understanding paleoenvironment, site organization, and fire use behaviours during the LGM in eastern Europe.

2 | Site Setting, Stratigraphy and Archaeological Context

Korman′ 9 is an Upper Palaeolithic site located on a northern facing terrace on the right bank of the Dniester River in Ukraine (Kulakovska et al. 2021). The site is in the archaeologically rich Middle Dniester region, which features several nearby archaeological sites of similar chronologies, namely Doroschivitsi III, Korman′ IV, Molodova I, and Molodova V (Chernysh 1977, 1987; Klein 1974; Kulakovska et al. 2021; Kulakovska et al. 2015; Noiret 2009)—see Figure 1. Figure 1B also includes additional Ukrainian sites with later Epigravettian occupations like Barmaky and Mezhyrich (Chabai et al. 2022; Haesaerts et al. 2015; Hoffecker 2005; Klein 1974; Kulakovska et al. 2015; Marquer et al. 2012; Soffer et al. 1997).

The Dniester River system is at the confluence of several waterways draining from the foothills of the Carpathians to the Black Sea. Within the section of the Middle Dniester valley, where Korman′ 9 is located, the Dniester River has incised layers of Cretaceous rocks including argillites, sandstones and limestones to the underlying Proterozoic stratum made up of siltstone, sandstones and argillites (Figure 2). The southern bank, where the site is located, is comprised of Miocene clay sandstones, siltstones and conglomerates. Across the river, the northern bank consists of Miocene sands, gritstones, conglomerates and tuffs. Currently this section of the Dniester is dammed and is part of a large reservoir lake, whose changing water table erodes the shoreline and banks intensely depending on the amount of yearly precipitation (Kulakovska et al. 2021).

The site of Korman′ 9 was found in 2012 during a survey of sites along the Dniester River. Excavations started the following year as part of the Middle Dniester Palaeolithic project within the

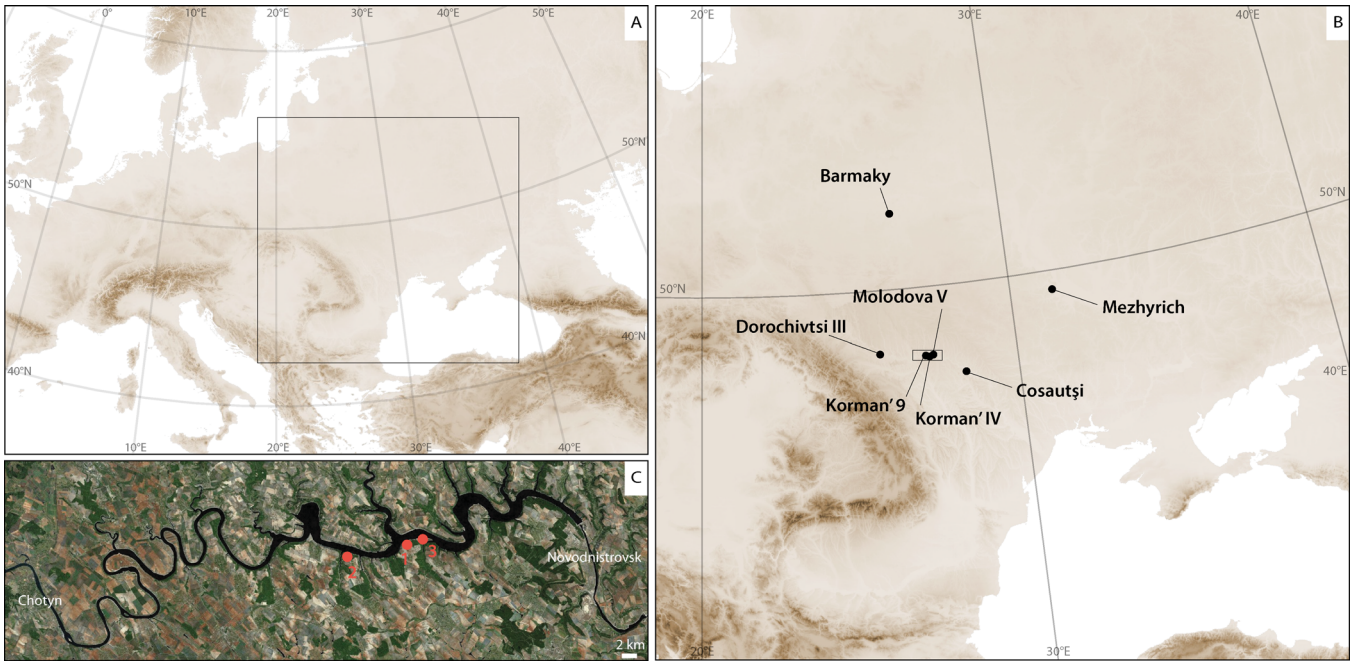

FIGURE 1 | (A) Map of Europe with the study area highlighted. (B) Map of study area with key LGM and Post-LGM sites with described combustion features highlighted. C) Onset map of Middle Dniester valley with the LGM sites of Korman' 9 (1), Korman' IV (3), and Moldova V (2) highlighted. Satellite image source: https://worldwind.arc.nasa.gov. Note the presence of a recent dam in C. Maps credit P.R. Nigst.

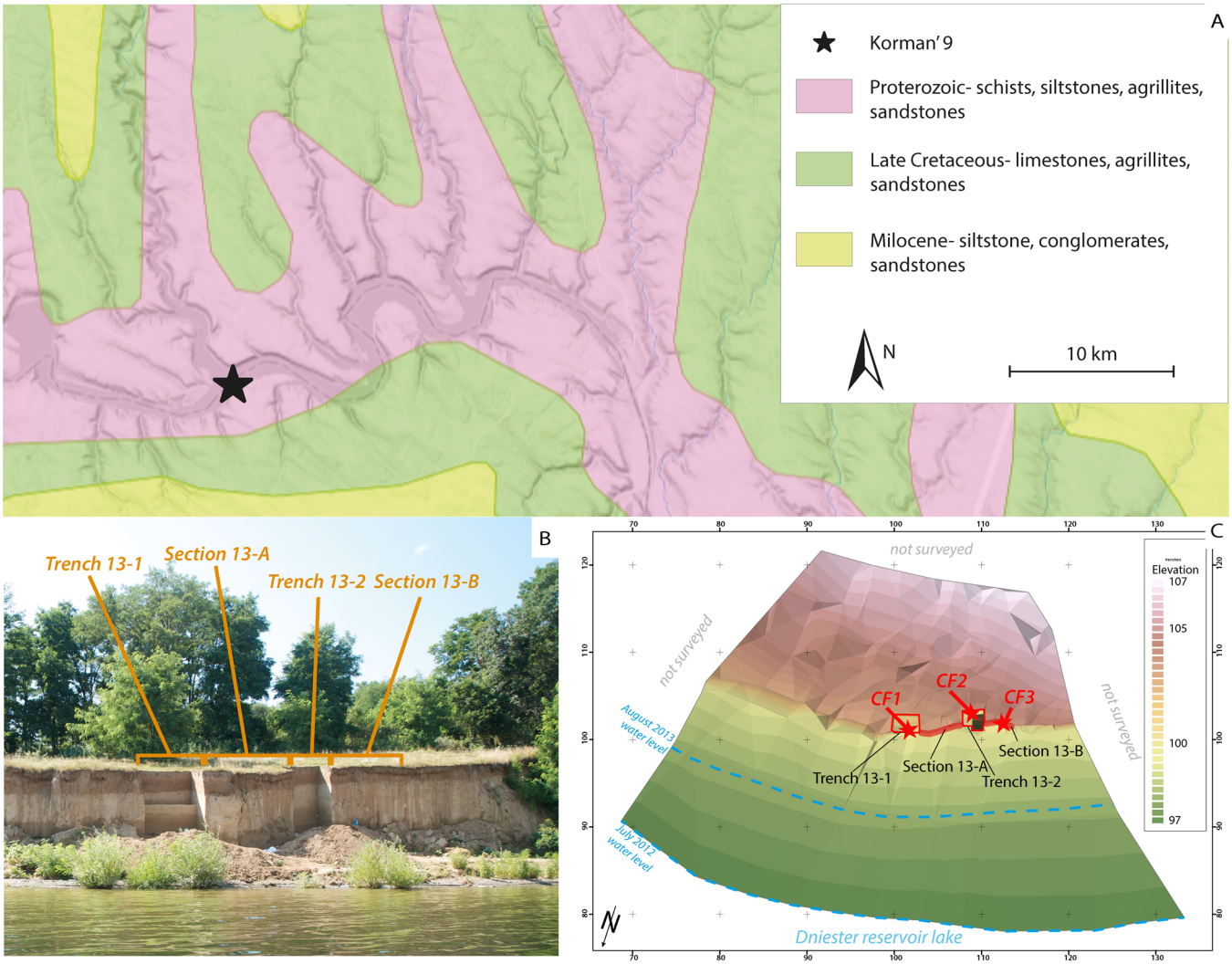

FIGURE 2 | (A) Geological map of the Middle Dniester Valley with Korman' 9 highlighted. Map source: Macrostrat (https://macrostrat.org/map/loc/27.1893/48.5749#z=8.7). (B) Site location on the Dniester River with the trenches and sections highlighted. (C) Digital elevation model for Korman'9 site. The locations of the combustion features are indicated by stars. Figure credit: W.C. Murphree & P.R. Nigst.

framework of the NEMO-ADAP project (Kulakovska et al. 2021). The site consists of ~50 m wide and roughly 4 m high cliff face incised into the southern slope of the valley (Kulakovska et al. 2021). A detailed overview of Korman' 9, including the site's stratigraphy, paleoenvironmental and archaeological remains was published by Kulakovska et al. (2021). Here, we will provide only a brief overview of the site's stratigraphy in direct relevance to the combustion features found at the site.

The site's stratigraphic sequence is composed of aeolian silts and silty sand lithostratigraphic units capped by the Holocene illuviated horizon (Kulakovska et al. 2021). The sequence can be subdivided into five distinct lithostratigraphic units which were further subdivided into subunits (SU), described in Figure 3. Korman' 9 features four archaeological layers (AL), from top to bottom: AL 0, AL I, AL II and AL III. AL I and II are associated with the Epigravettian and AL III with most likely Gravettian stone tool industries (Kulakovska et al. 2021). In total, three combustion features were discovered during the 2012 survey and the 2013 excavations at the site. Two of the combustion features, referred to henceforth as CF1 and CF2, were found within trenches 13-1 (CF1) and 13-2 (CF2) and are associated with AL I and the Epigravettian occupations at the site with an age between 22,167 and 21,398 cal BP (IntCal20, OxCal 4.4, 99.7% probability) (Kulakovska et al. 2021)—Figure 3. There is evidence of burning in both the lithic and fauna collections of AL I (Bosch et al. 2024; Kulakovska et al. 2021; Kulakovska et al. 2019). The third combustion feature, CF 3, was identified during cleaning of section 13-B and is associated with AL II, dated to between 22,645 and 22,086 cal BP (IntCal 20, OxCal 4.4, 99.7% probability) (Kulakovska et al. 2021). The dating of both AL I and AL II places the Epigravettian occupations at the middle of the LGM during both cold stadial conditions (AL II) and medium cold interstadial conditions (AL I) (Kulakovska et al. 2021, 248).

As outlined by Kulakovska et al. (2021), the archaeological work at the site followed state-of-the-art excavation methodology and techniques to collect high- resolution lithostratigraphic provenience and piece plotting of artefacts. For the combustion feature CF1, several vertical sections were made to better observe the deposits in several cross-section profiles.

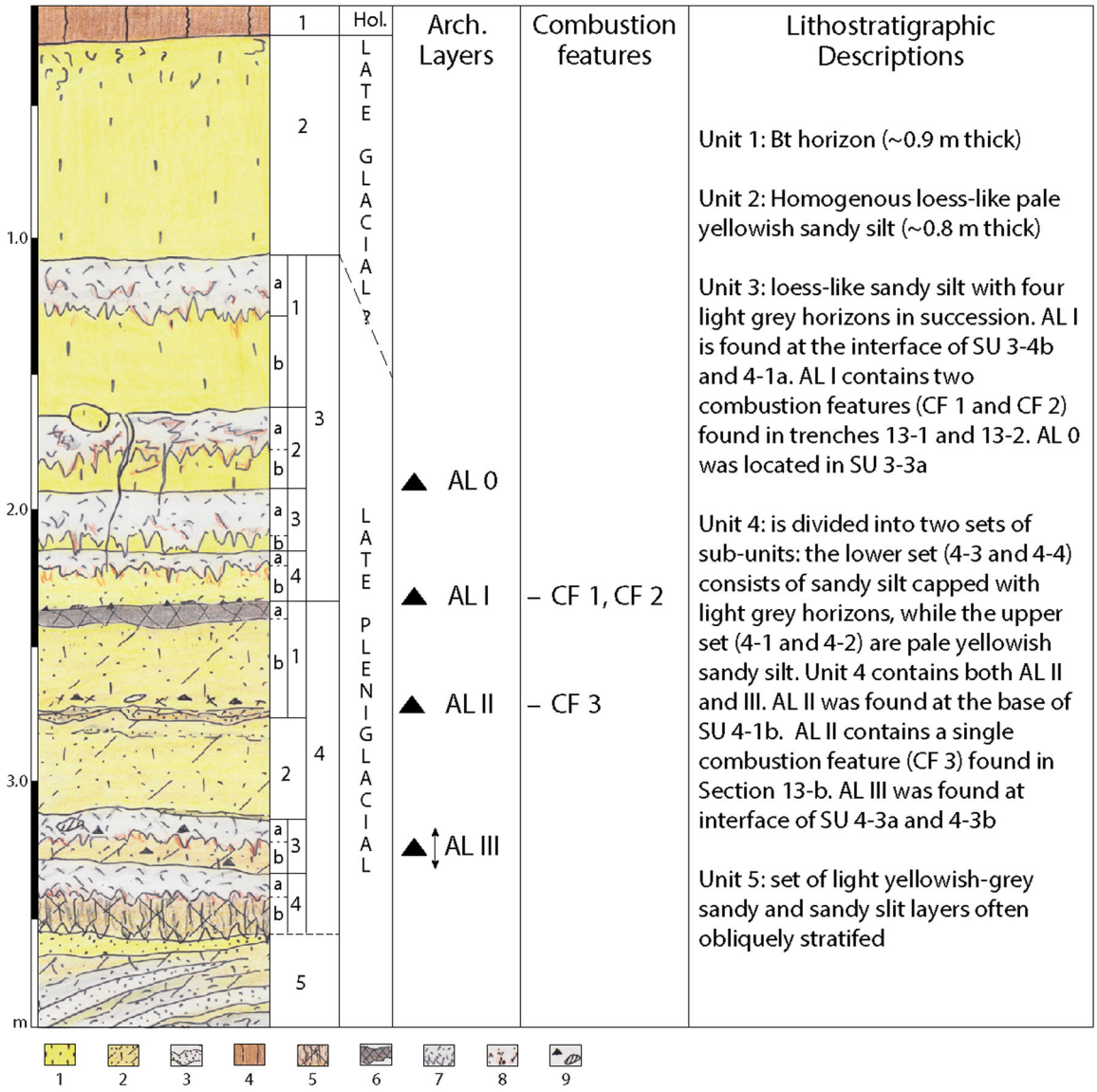

FIGURE 3 | Lithostratigraphy of Korman' 9 with the location of the archaeological layers, combustion features and lithostratigraphic descriptions on the right. 1: silt; 2: sandy silt; 3: sand; 4: Bt horizon; 5: bioturbated horizon; 6: humic lenses; 7: grey silt (tundra gley); 8: iron staining; 9: lithic artefacts and faunal remains. Abbreviations: AL: Archaeological Layer. Hol.: Holocene. Figure credit: P.R. Nigst and W.C. Murphree, Stratigraphic drawing: P. Haesaerts, S. Pirson and P.R. Nigst.

3 | Methods

To describe and examine the combustion remains at Korman' 9, we employ a multiscale descriptive criterion for combustion features based on the methods proposed by Mallol et al. (2017) and Murphree and Aldeias (2022). These include the following macro- and microstratigraphic descriptors: feature shape and dimensions; the presence and descriptions of ash (white layer), black (burned topsoil and charcoal) and red (rubified substrate) layers; the presence of superimposed layers or stacking; micro-observations such as the microstratigraphy of the combustion features and its contents as well as the degree of preservation of the combustion remains. For shape descriptions, we employ the nomenclature for contained combustion features proposed by Mallol et al. (2017). The macro-observations of the combustion features at Korman' 9 were collected from field and excavation drawings, photographs and field notes. We also created high-resolution photogrammetry models utilizing the Agisoft Metashape program, version 1.7.5 (Agisoft 2021) using photographs from the different phases of excavation of the features. The number of photographs varied based on availability for each section or excavation phase (see Supporting Information S1: Table 1). The settings used in Agisoft Metashape for the model production and georeferencing are described in the Supporting Information. Our descriptions also include soil micromorphological observations and methods of colorimetric analysis for estimating temperature (Figure 4) described in the sections below.

3.1 | Soil Micromorphology

The micromorphological analysis is based on six micromorphological samples taken from CF1 and CF2 during the 2013

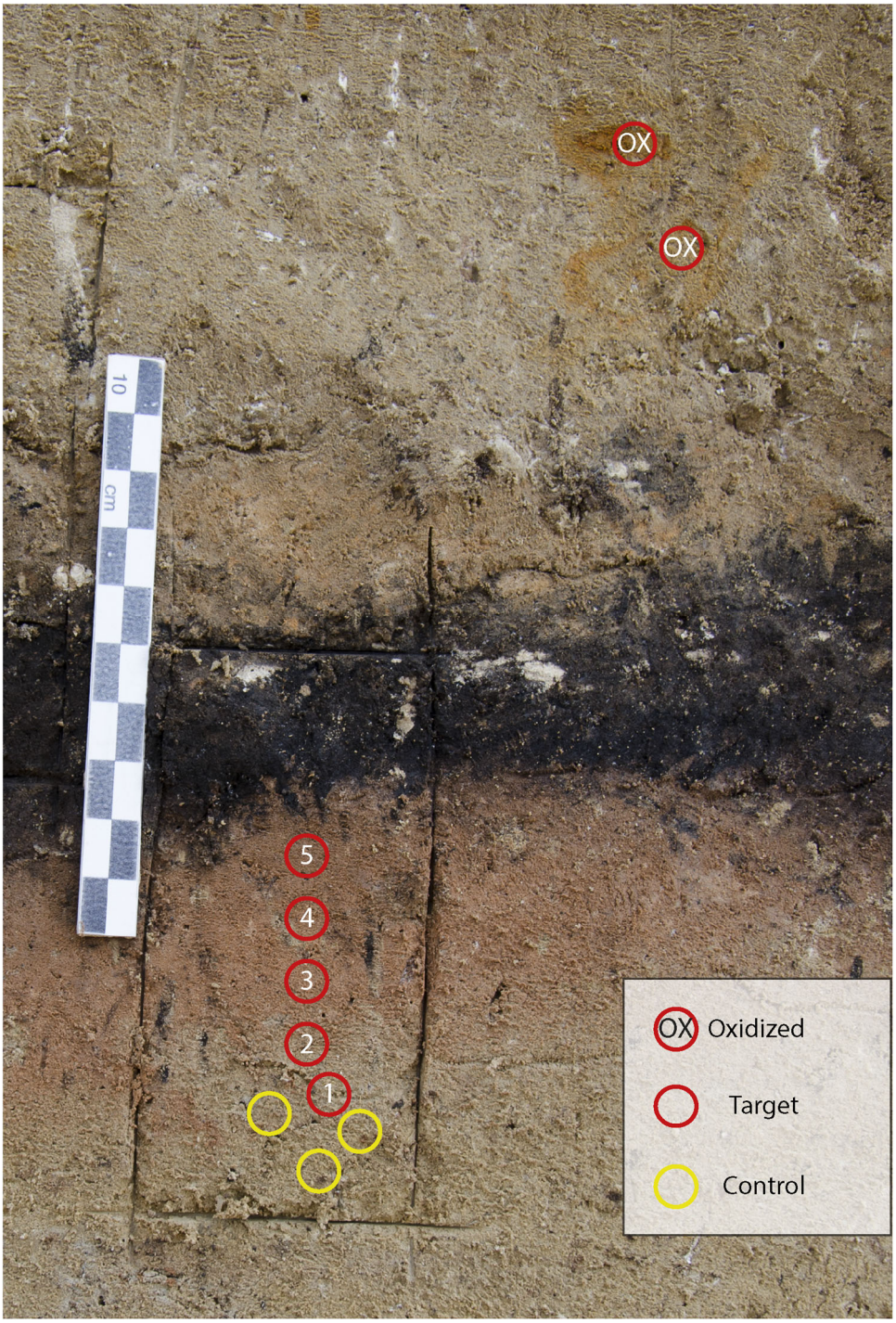

FIGURE 4 | Colorimetric analysis for CF1. Location of the target (red circles), control (yellow), and oxidized sediments (OX) characterized in the analysis. Note the white mottles in the sediments corresponding to secondary Ca precipitates, and the orange colours, which correspond to higher amounts of Fe oxides.

field season by one of us (PRN). In total, four samples were taken from CF1, labelled: Soil Micromorphology (SM)-01, SM-02, SM-04 and SM-05, along with a control sample SM-03 taken ~30 cm laterally to the west from samples SM-01 and SM-02 (Figure 5). A single sample (SM-09) was taken from CF2. Samples SM-01 and SM-04, as shown in the figures below, were fractured during transport from Ukraine to the laboratory facilities at the Charles McBurney Laboratory for Geoarchaeology at the University of Cambridge (UK). The block samples were hardened using a standardized mixture of 1800 ml of crystic Polyester resin mixed with 200 mL of acetone and 1.0 mL of Methyl Ethyl Ketone catalyst (MEKP). The samples were then placed within a vacuum chamber to dry before thin section production. The resulting thin sections are 10×6.5 cm in size and are roughly 30 μm thick. Additional thin sections of blocks SM-04 and SM-05 were reproduced by Spectrum Petrographic (Vancouver, USA). The thin sections from Spectrum Petrographic are 7.5×5 cm in size and 30 μm thick. All thin sections were scanned with an Epson flatbed scanner using 3200 dpi

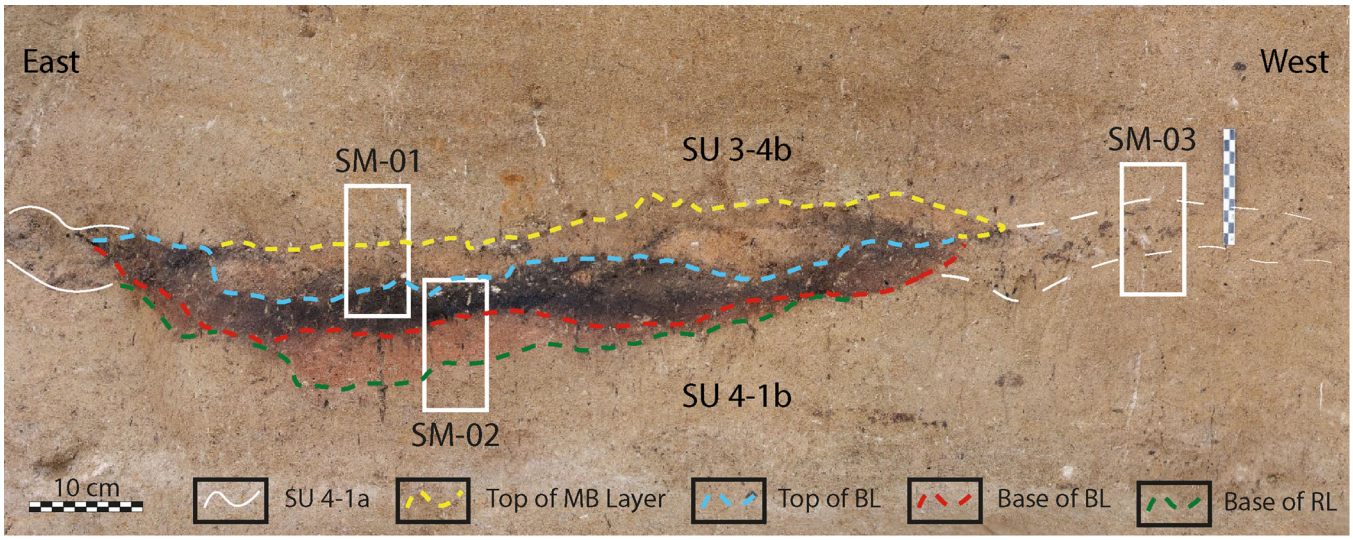

FIGURE 5 | Korman' 9, Trench 13-1, AL I, CF1: Annotated orthophotograph of the CF1 based on the Phase 0 model (cleaned section before excavation). Scale is 10 cm. The white boxes show the location for soil micromorphology samples (SM-01, SM-02 and SM-03). The extent of SU 4-1a is shown in the white lines. SU 4-1a becomes less visible further to the west as indicated by the dashed white lines. The four coloured dashed lines indicate the different contacts between the deposits of the combustion feature: yellow = top of the mottled brown (MB) deposit, light blue = top of the black layer (BL), red = the base of the BL and the green indicates the base of the red layer (RL).

resolution and RGB photometric interpretation. The sections were then studied under a Nikon stereoscopic microscope (Eclipse SMZ25/with camera Fi3Binocular) under magnifications from 0.5 to x200 and under a Nikon petrographic microscope (LV100ND with Ds/Ri2 Camera) at magnifications ranging from 20 to x400 in Plane-polarized and Cross-polarized light (PPL, XPL, respectively) at the Microscopy Laboratory 'MICROLab' at Interdisciplinary Center for Archaeology and the Evolution of Human Behaviour (ICArEHB), University of Algarve (Portugal). Micromorphological descriptions and nomenclature follow Stoops (2003).

3.2 | Colorimetric Analysis

We employed a method for thermal characterization of combustion remains using digital photographs. In a previous paper, Ferro-Vázquez et al. (2021), proposed a systematic method for the identification of archaeological heated sediments based on the instrumental measurement of colour in the CIELab system. This method consisted in the study of the colour of sediment samples heated under controlled conditions using a benchtop colorimeter to characterize the change in colour derived from mineralogical and physiochemical transformations of the sediments when heated, leading to the production of haematite. Through discriminant analysis of colour data, the authors produced equations capable to accurately classify unknown samples as burnt or unburnt and, for those burnt, provided an estimation of the heating temperature to an accuracy that depended on the chemical and mineralogical composition of the sample (Ferro-Vázquez et al. 2021).

Here, we apply the methods and calculations from that study to digital photographs of CF1 (see detailed methods in Supporting Information) to obtain temperature estimations. Digital images contain large amounts of data, collected by means of simple, cheap, fast and less laborious techniques than conventional soil and sediment analyses. The use of digital cameras (including built-in mobile phone cameras) has been proposed by various studies as soil-colour sensors (e.g., Aydemir et al. 2004; Fan et al. 2017; Heil et al. 2020; O'Donnell et al. 2011; Rossel et al. 2008). The work from Levin et al. (2005) demonstrated that it is possible to obtain information on the chemical and physical properties of soils and sediments through the analysis of the colour of images taken with a standard digital camera in natural daylight, without any previous knowledge about the camera's characteristics, and with data acquisition and analysis based on commercially available software. Within the archaeological discipline, recent works by Haburaj et al. (2019) and Haburaj (2021) have used RGB colours from digital photographs for helping in the definition of stratigraphic layers, based on the correlation of RGB data with soil and sediment properties.

The photograph of CF1 was taken in late July 2013 in sunny weather conditions and > 30°C temperature. The section was freshly cleaned and wet. At the time of photographing, the north-facing section was in the shade. CF 1 (Figures 4 and 5) sits on SU 4-1a, which is assumed to be thermally modified producing a burned organic-rich black layer as well as an area of red-orange heated materials immediately below it corresponding to SU4-1b. Three sectors of the photograph assumed to be unheated, and representative of the average composition and weathering conditions of the site were selected as control (yellow circles), shown in Figure 4. In that regard, the parts of the photograph showing white colours were interpreted as concretions of Ca compounds. Such areas were avoided in the selection of the control locations since they were judged not to be representative, and since in this method, we aim to characterize Fe oxide transformations upon heating rather than Ca-related colour changes. A sequence of five points (red circles) at different distances of the combustion feature was also

characterized, with the intention to capture the redder colours, thus the increase in temperature, in the sediment layers closer to the combustion feature (Figure 4). Two additional points (labelled ox) above the combustion feature (Figure 4) were sampled to test the capacity of the method for discriminating between reddish colours produced by temperature from those produced by weathering and reduction-oxidation processes.

Although the detailed analytical composition of the Korman'9 sediments is not available, it is known that they consist of loess type materials with variable amounts of Fe oxides and secondary Ca compounds. The latter are irregularly distributed throughout the profile (see Figure 4). Therefore, two of the seven compositional groups (CA) proposed in Ferro-Vázquez et al. (2021) were used for assessing the presence of heating and the temperature reached. The CA3 cluster corresponded to felsic silicate samples, with low Ca contents and moderate total Fe concentrations (1%–2%), with 30%–50% of the Fe in secondary. The CA6 consisted of samples from soils of calcareous composition that have different amounts of total Fe and Fe oxides but with high or very high amounts of Ca, and with most of their carbon being in inorganic pedogenetic forms.

4 | Results

The results of our analysis for CF1 and CF2 are subdivided into macro- and micro-observations sections. Additionally, we present the results of colorimetric analysis for CF1 in the section below. CF3 was left unexcavated and only macrostratigraphic descriptions are available.

4.1 | Combustion Feature 1

4.1.1 | Macroscopic Descriptions

CF1 is an unlined open flat combustion feature. The combustion feature is located at the surface of SU 4-1a, which consists of a highly bioturbated light brown silt exposed in excavation trench 13-1. Field observations, as well as paleoenvironmental markers (e.g., microfauna remains and sedimentary/pedogenic signatures) characterize SU 4-1a as a well-watered pedogenesis horizon associated with landscape stabilization during an interstadial event of sub-arctic cold conditions (see Kulakovska et al. 2021). SU 4-1a becomes more diffused towards the west of the combustion feature. This SU overlies SU 4-1b and is below SU3-4b. Both SU 4-1b and SU3-4b consist of pale ochre yellowish loess-like sandy silt. Based on field observations by Kulakovska et al. (2021, 235), CF1 consists of three distinct deposits starting from the bottom to the top: a red layer (RL), a black layer (BL) and finally an overlying greyish or mottled brown (MB) deposit above (Figure 5). The RL has a maximum thickness of 4.6 cm and is approximately 70 cm in diameter. The BL has a maximum thickness of 4.4 cm and maximum extent of 1.0 m in length, based on measurements in Agisoft based on the model of the excavation phase 0 (Figure 5). Based on field observations, there is no clear evidence of superimposed combustion features or stacking (i.e., re-use of the same approximate location for several, discernible subsequent firing features). The undulating and convoluted nature of the deposits and their presence of a slope points to the effects of solifluction partially affecting the combustion feature deposits (Figure 6).

4.1.2 | Micromorphological Descriptions (Samples SM-01, SM-02, SM-04, and SM-05)

Based on observations from micromorphology samples SM-01 (Figure 7) and SM-02 (Figure 8) taken from Phase 0 of the excavation (Figure 5), CF1 consists of three distinct deposits with SU 3-4b above and SU 4-1b below. These deposits include from bottom to top: a RL, a BL and a MB deposit. The matrix of the underlying unaltered SU 4-1b is a homogenous light yellowish brown well-sorted silt with few, very fine, subangular sand-sized quartz grains, and few rounded glauconite grains. SU 4-1b has a generally massive microstructure with no separated peds and few voids (Stoops 2003). The groundmass is calcitic crystallitic with some domains of mosaic speckled b-fabric, with generally regular vughs and chambers, some of which have hypocoating of secondary carbonates associated with plant root casts (rhizoliths). The basal deposit of the combustion feature consists of the rubified thermally altered 4-1b called the RL. The RL (Figure 8) is a homogeneous reddish silt with fine sand-sized subangular quartz grains. RL has a weakly developed lenticular and vughy microstructure (Figure 8I). There are also isolated domains of granulated microstructures nearer the interface between the RL and unaltered 4-1b. The matrix contains of very few small, rounded mollusc shell fragments ~250 μm in size (Figure 8J), as well as burnt plant remains directly associated with burrowing from soil fauna/flora (Figure 8H). The contact between the unaltered and thermally altered 4-1b (RL) is diffused with no sharp contact. Near the contact between the RL and subunit 4-1b, the RL has a weakly developed platy/granular structure (Figure 9A) in comparison to subunit 4-1b, which has a generally massive microstructure. There is evidence of inverted grading between peds in subunit 4-1b (Figure 9B) like what is described by Van Vliet-Lanoë (2010, 88) in similar sediments after the collapse of lenticular or platy microstructures.

The RL has a sharp contact with the overlaying BL with localized bioturbation. The BL is a black, dense organic-rich silt deposit with a spongy microstructure. The BL likely corresponds with mixture of thermally altered 4-1a (humic horizon) and combustion materials. The deposit has abundant burned plant remains as well as few small, sand-sized burned bone fragments. These range from partially carbonized, shown in Figure 7I (green arrows), to fully carbonized (shown in Figure 7J (green arrows) (Ellingham et al. 2015). The BL also has burned undefined minute organic material (Figure 8G) and small (~1 mm sized) ash aggregates (Figures 8E,F,G). No calcined bone was identified in the micromorphological samples SM-01 or SM-02. Some of the charcoal and plant remains are humified and/or partially burned (Figure 8D). The upper deposit of the combustion feature consists of mottled brown (MB) fine-grained silt with fine- grained sand-sized subangular quartz grains. The contact between the BL and overlying MB deposit is diffused with clear mixing at the contact between the two deposits. The MB deposit is organic-rich with a vughy microstructure, as well as some channels and domains of vermicular microstructure derived from soil fauna such as earthworm burrowing (Stoops 2003). The matrix has small, rounded clay

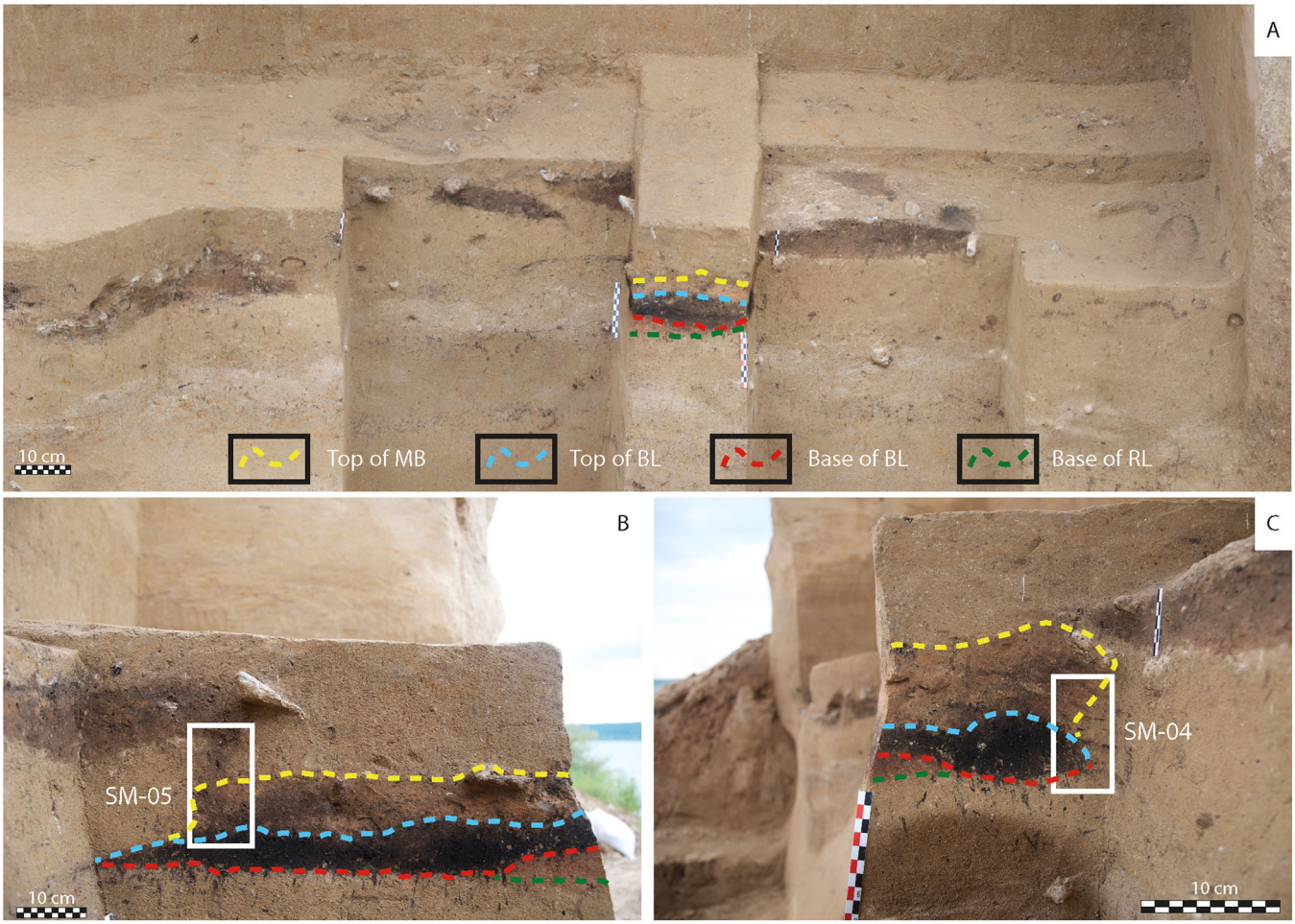

FIGURE 6 | Korman' 9, Trench 13-1, AL I, CF1: (A) Orthophotograph of CF1 model during Phase 3 of the excavation (after the removal of SM-01, SM-02 and SM-03 and exposure of new sections). The dark brown patches visible in the section are solifluction lobes. The two lower photographs show the left (B) and right (C) profiles of CF1. Model created by W.C. Murphree; photographs by P. R. Nigst. Scale in each photo is 10 cm. The white boxes indicate the sample location of micromorphology samples SM-05 (B) and SM-04 (C). The four dashed lines indicate the different deposits of the combustion feature: yellow = top of the mottled brown (MB) deposit, light blue = the top of the black layer (BL), red = the base of the BL and green indicates the base of the red layer (RL).

aggregates, as well as very few cm-sized carbonate nodules. Some of the aggregates have clear capping (Figure 7E). The contact between the MB deposit and SU 3-4b above is diffused (Figure 7). SU 3-4b has a similar composition to SU 4-1b except with the presence of very few small carbonate nodules (so-called loess dolls), shown in Figure 7C,D. SU 3-4b has a generally massive microstructure with few voids. Overall, the two micromorphological samples associated with CF1, phase 0, show extensive bioturbation with localized mixing of the BL and RL of the combustion feature as well as between the RL and SU 4-1b sediments (Figures 7 and 8).

Micromorphological samples SM-04 and SM-05 were taken during Phase 3 of the excavation of CF1 (Figure 6). Both deposits are affected by solifluction with clear overthrow. The RL is not present in either sample.

SM-04 consists primarily of the edge of the combustion feature (Figures 6 and 10). In this sample, the basal deposit, SU 4-1b, has a generally massive microstructure with no separated peds and few void spaces. In this sample, there is a direct contact between SU 4-1b and MB layer which is diffused with mixing via bioturbation. There is a lens of the BL within the MB layer with a diffused lateral contact between the two deposits (Figure 10AD). The BL in sample SM-04 has a spongy microstructure with abundant channel voids and vermicular structures from soil fauna burrowing or plant roots. The deposit is organic-rich with abundant burned and partially burned plant remains (Figure 10H). On the upper slide (Figure 10A,C) the MB deposit is deformed by solifluction, there is a domain of irregular diffused contact with SU 3-4b. The MB deposit has a vughy microstructure with nonconnected vughs and chamber voids. This deposit contains rounded aggregates of SU 3-4b and rubified sediment.

The deposits sampled in SM-05 are again clearly affected by solifluction. The lower thin section shows a sharp contact with isolated mixing between the BL and the overlaying SU 3-4b (Figure 11B,D). The BL deposits have a generally spongy microstructure with clear evidence of bioturbation (Figure 11D), containing both burned and unburned bone fragments as well as charcoal fragments (Figure 11H). In the lower section, SU 3-4b has a generally massive microstructure with few channel voids and vughs. The upper thin section (Figure 11A,C) contains a diffused SU 3-4b with domains of MB. Here, SU 3-4b has a complex microstructure, which is generally massive with domains of vughs and channel voids

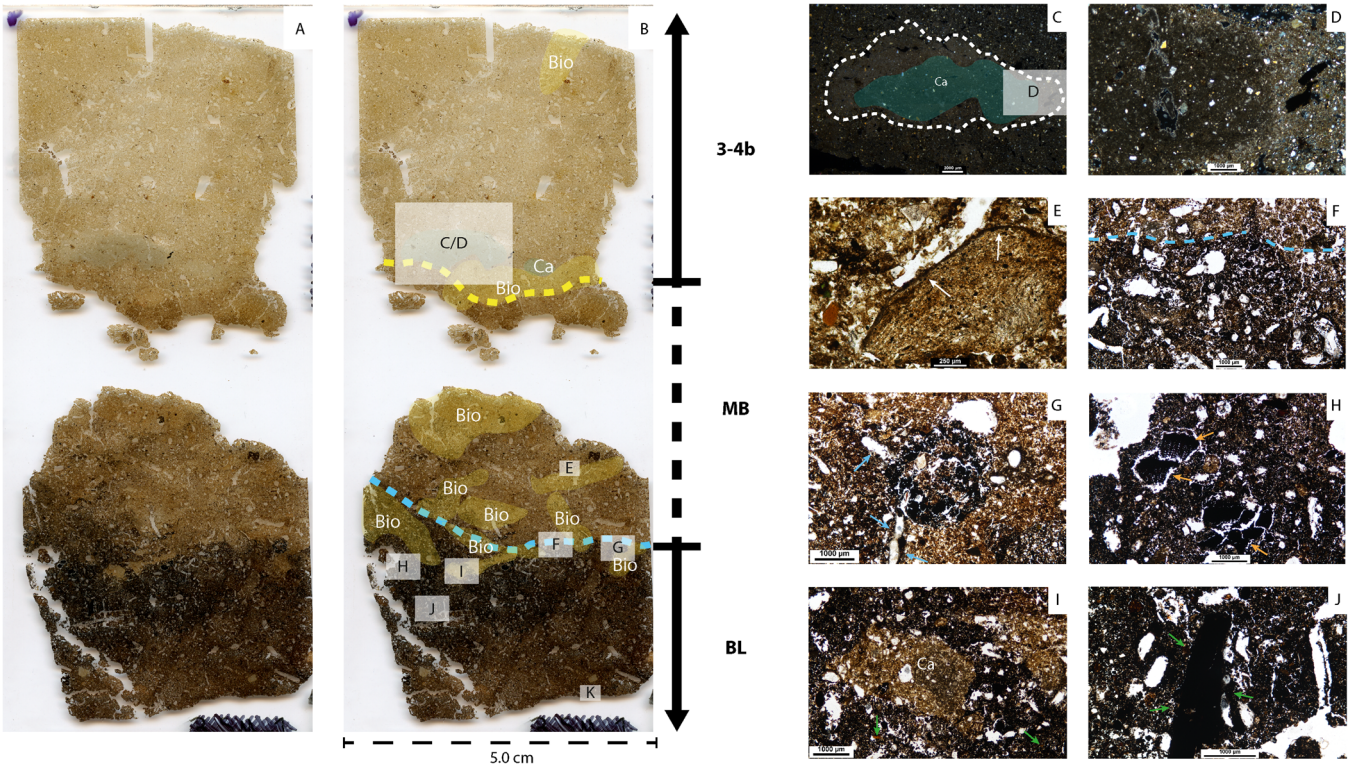

FIGURE 7 | CF1 from Korman' 9, Trench 13-1, AL I: Thin sections and photomicrographs taken from SM-01 corresponding to CF1. (A) the original thin section produced for SM-01. Note that the thin section was broken during transport before impregnation, hence the gap between the upper and lower deposits. (B) Same thin section with the annotated contact of SU 3-4b, the MB deposit (yellow line), MB and BL (light blue line). Bioturbated (Bio) domains are highlighted in yellow, while calcium carbonate nodules (Ca) are highlighted in blue. Locations of photomicrograph are marked with the white transparent boxes. (C) Calcium carbonate concretion or 'Loess Dolls' (highlighted in blue and labelled Ca) with carbonates leaching into the surrounding sediment (extent indicated by the white dotted line) shown in cross-polarized light (XPL), scale is 2000 μm. (D) Close up of the 'loess doll' with carbonates leaching in the surrounding substrate, XPL, scale is 1000 μm. (E) Capping (white arrows) on top of an aggregate within the MB deposit, Plane Polarized Light (PPL), scale is 250 μm. Cappings are common features in freeze-thaw related processes. (F) Charred organic remains at the interface between MB and BL (blue line), PPL, scale is 1000 μm. G) Charred organic remains found within the MB/BL contact, PPL, scale is 1000 μm. Note the common channels associated with bioturbation (blue arrows). (H) Burned plant remains (light orange arrows) and spongy, very porous microstructure with abundant, vesicles, vughs and channels found within the BL, PPL, scale is 1000 μm. The BL has abundant vesicles, channels, and highly interconnected vughs throughout the matrix. (I) Calcium carbonate concretion (Ca) found within the BL, PPL, scale is 1000 μm. Note the lack of capping over the concretion. (J) Fully carbonized bone within the BL, PPL, scale is 1000 μm.

(Figure 11A,C). Some of the channel voids are infilled with microcrystalline carbonates or micrite (Figure 11F). In the upper thin section, the diffused SU 3-4b deposit contains burned bone fragments, including one with an embedded lithic fragment (Figure 11I,J). The presence of an embedded flint flake in a bone clearly attests to human processing of this faunal remains. The mixing of anthropogenic materials (such as the burned bone with the embedded lithic) along with the isolated domains of MB deposits within the more geogenic deposits of SU 3-4bare likely derived from repeated solifluction events over time. The domains of MB materials are distinguishable due to colour and composition variations that derived from the relatively higher presence of sand-sized partially burned bone fragments (Figure 11E) and charcoal remains.

4.1.3 | Colorimetric Analysis

The results of the colorimetric analysis of a digital photograph of CF1 used equations to assess if the sediments were heated, namely comparing the results to two sediment groups described in Ferro-Vázquez et al. (2021): CA6 (which considers sediment composition with high amounts of Ca) and CA3 (which corresponds to felsic silicates with low amounts of Ca). Applying both types of equations, the Korman' 9 sediments up to 5 cm below the BL of CF 1 were assigned as heated when compared with the control sediments (Figure 12 and see Supporting Information for data and calculations for CA6 equations). Then, we have chosen to use the equations of CA3 to further estimate to what temperatures these sediments might have been heated. This choice relies in the fact that, although Korman' 9 sediments have indeed certain amount of secondary Ca precipitates (consisted with CA6 type of sediments), such compounds are unevenly distributed as mottles and concretions (see white mottles in Figure 12) and are not the main components of the overall sedimentary matrix. In this regard, both the control and the target locations for CF1 colorimetric analysis were chosen avoiding white areas of the photograph, in a sampling strategy addressed to characterize Fe oxide transformations and not Ca-related colour changes. The CA3 equations results show that, from 2–5 cm of distance from the BL, the sediments have been heated enough to produce mineralogical transformations and colour change. Temperatures of 200°C were reached at a

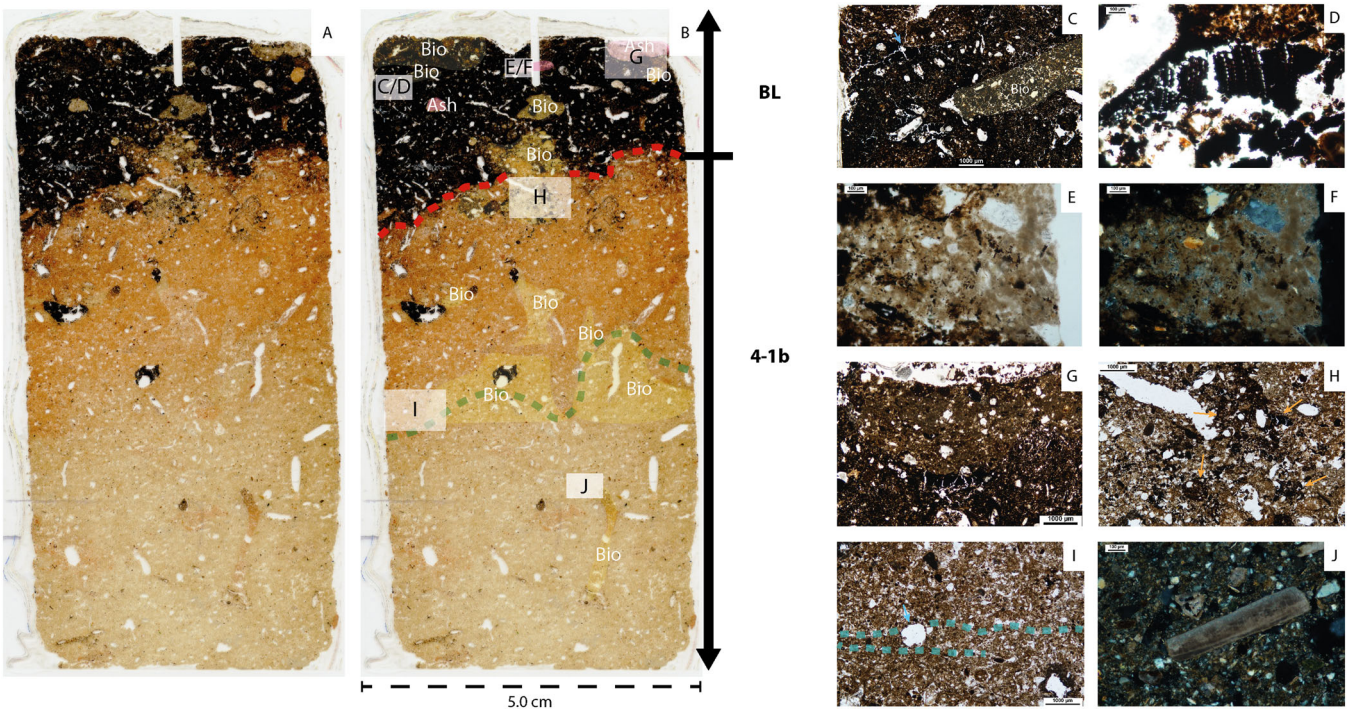

FIGURE 8 | CF 1 from AL I in Trench 13-1: Thin sections and photomicrographs taken from SM-02. (A) The original thin section scans produced for SM-02. (B) Annotated thin section with the contacts between BL and RL (thermally altered SU 4-1b) (red line) overlying the unrubefied SU 4-1b sediments (green line). Bioturbated domains (Bio) are highlighted in yellow, and ash-rich domains (Ash) are highlighted in pink. Photomicrograph locations are shown in the white boxes. (C) Photomicrograph of burned plant remains found within the BL, PPL, scale is 1000 μm. Some of which (blue arrow) appear to be broken via frost action. Vermicular structures from soil fauna burrowing are highlighted in yellow. (D) Close up view of a charcoal shown in Figure 8C, PPL, scale is 100 μm. Note that the remains appear to be humified and not fully carbonized. (E) and (F) Small isolated ash domain found within the BL, in PPL (E) and XPL (F), scale is 100 μm. (G) Preserved ash domain within the BL, PPL, scale is 1000 μm. (H) Burned plant and organic remains (orange arrows) mixed within the RL due to bioturbation, PPL, scale is 1000 μm. (I) Weakly developed laminar/granular microstructures (light blue lines) and vesicles (blue arrow) associated with freeze-thaw affecting RL deposits, PPL scale is 1000 μm. (J) Shell fragment within SU 4-1b, XPL, scale is 100 μm.

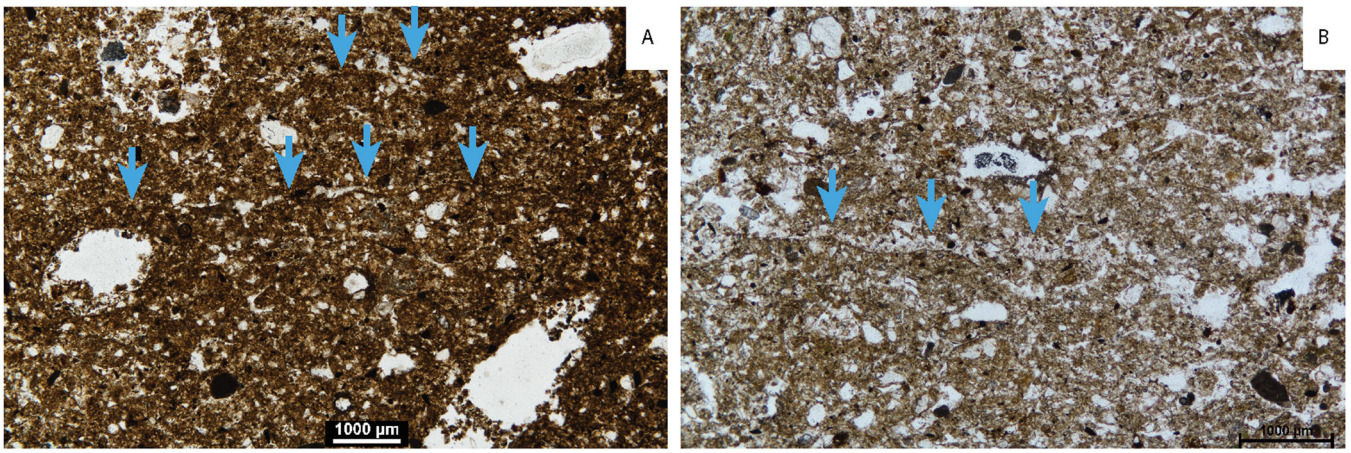

FIGURE 9 | Photomicrographs from the RL and SU 4-1b in sample SM-02 showing the effects of cryoturbation. (A) Domain of granulated microstructure within in RL deposit with cappings indicated by the blue arrows, PPL, scale is 1000. (B) Inverse grading (blue arrows) where the underlying silt capping is covered with coarse grain materials potentially derived from collapsed lenticular microstructures.

distance of 5 cm (sample location 1, Figure 12A), with temperatures of 500°C at 3 cm (sample location 3, Figure 12-A) and 600°C at 2 cm (sample location 4, Figure 12A) (see Supporting Information for data and calculations). These results are consistent with previous experimental studies by Aldeias et al. (2016) on loess-like sediments, in which a temperature of 600°C at 2 cm of depth was reached after heating the sample at a temperature of 950°C during at least 3 h. It is relevant to note that, in our calculations for the sediment at 1 cm below the BL (sample location 5, Figure 12A), which would be the location expected to be heated at higher temperature given the proximity to the combustion event, results show a lower calculated temperature (approx. 300°C). However, it

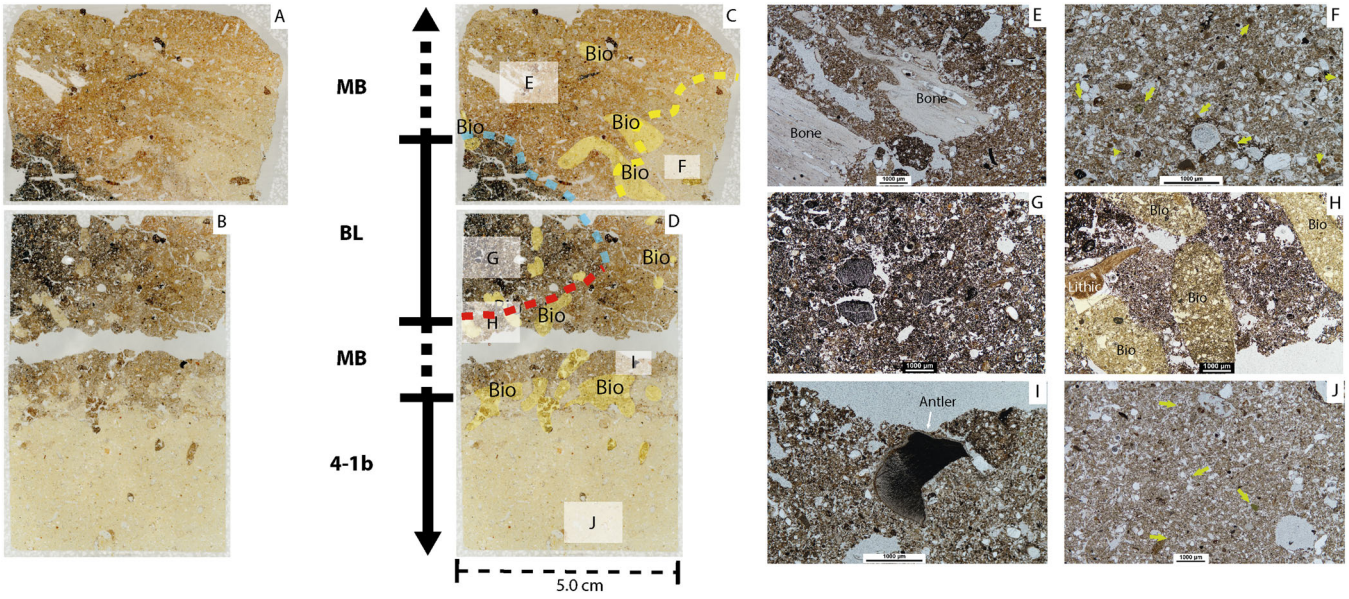

FIGURE 10 | CF1, AL I, Trench 13-1: Thin sections and photomicrographs taken from sample SM-04. Sample location shown in Figure 7C but further back into the section. Sections (A) and (B) are thin sections scans produced by Spectrum Petrographic. Sections (C) and (D) are the same image with annotations of the interfaces between MB and SU 3-4b deformed by solifluction (yellow line), MB and BL (light blue line) and RL (red line). Bioturbation (Bio) is highlighted in yellow, and the location of the photomicrographs shown to the right are indicated by the white boxes. (E) Photomicrograph of unburned bones found within MB deposit (SU 4-1a), PPL, scale is 1000 μm. (F) Photomicrograph of matrix of area marked in (c) showing of SU 3-4b showing moderately sorted with a common sand to fine sized quartz grains, massive microstructure with few void spaces, common silt-sized glauconite grains (yellow arrows) PPL, scale is 1000 μm. (G) Spongy microstructure of BL with abundant charcoals, PPL, scale is 1000 μm. (H) Partially burned lithic fragment within the MB deposit, bioturbation (highlighted in yellow) and contact with BL (demarked by the redline, PPL, scale is 1000 μm. (I) Partially burned bone/antler found within the MB deposit near the interface with the underlying SU 4-1b, PPL, scale is 1000 μm. (J) Well-sorted generally massive microstructure of the underlaying SU 4-1b, PPL, scale is 1000 μm. Glauconite grains are marked by light green arrows.

is clear that this part of the profile is stained with black organic particles from the BL deposit above it, which changes the values of L^*, a^* and b^*. Consequently, measurements at this location provide inaccurate temperature estimations and will thus not be considered for archaeological interpretations.

4.1.4 | Micromorphological Description of SM-03

This sample was taken 30 cm to the west of phase 0 CF1 (Figure 5). The sample contains loessic materials from SU 3-4b and SU 4-1b with lenses of bioturbated SU 4-1a materials. The basal layer 4-1b is as described in the sections above, along with some domains of weakly developed lenticular microstructures. 4-1b has very few vughs and channel voids some of which are infilled with secondary carbonates (Figure 13G). The overlying SU 3-4b is a dense well-sorted silt with lenses of bioturbated organic-rich silt (likely 4-1a) as shown in Figure 13B,C. The 3-4b has a complex microstructure with more granular microstructures near the interface with 4-1b, as well as domains of weakly developed lenticular microstructures. The SU becomes more massive towards the top of the sample.

4.2 | Combustion Feature 2

4.2.1 | Macroscopic Descriptions

CF2 is an unlined open flat combustion feature based on the nomenclature proposed by Mallol et al. (2017). The feature is located on top of SU 4-1a in excavation trench 13-2 (Figure 14), where it is affected by solifluction. The base of SU 4-1a has sharp contact with 4-1b. Above this contact there is max. 2–3 cm thick SU 4-1a with AL I located on its top. CF2 is located at the same position. The overlying ~10 cm of sediment is a solifluction affected sequence of lenses of SU 4-1a interstratifying yellowish loessic sediment (either SU 4-1b or SU 3-4b). CF2 is roughly 82 cm in maximum diameter and roughly 3.5 cm in maximum thickness based on the model produced in Agisoft Metashape (Figure 14). However, the feature is likely deformed by solifluction. There is a thin ash layer, described by Kulakovska et al. (2021, 235) directly above the combustion feature, which overlays the BL and rubified (RL) layers that were clearly visible in the field. This layer likely corresponds to the MB layer described in the section below. Based on the model of CF2, the BL is 1.5 cm in maximum thickness while the RL is approximately 2 cm in maximum thickness. There is no visible evidence of stacking or superimposed combustion features.

4.2.2 | Micromorphological Descriptions (Sample SM-09)

CF2 has a single micromorphological sample SM-09 taken from trench 13-2 (Figures 14 and 15). SM-09 contains three distinct deposits related to the CF2: RL, BL and MB (Figure 15). The section of SU 4-1b beneath CF2 has a complex microstructure with domains with no separated peds and

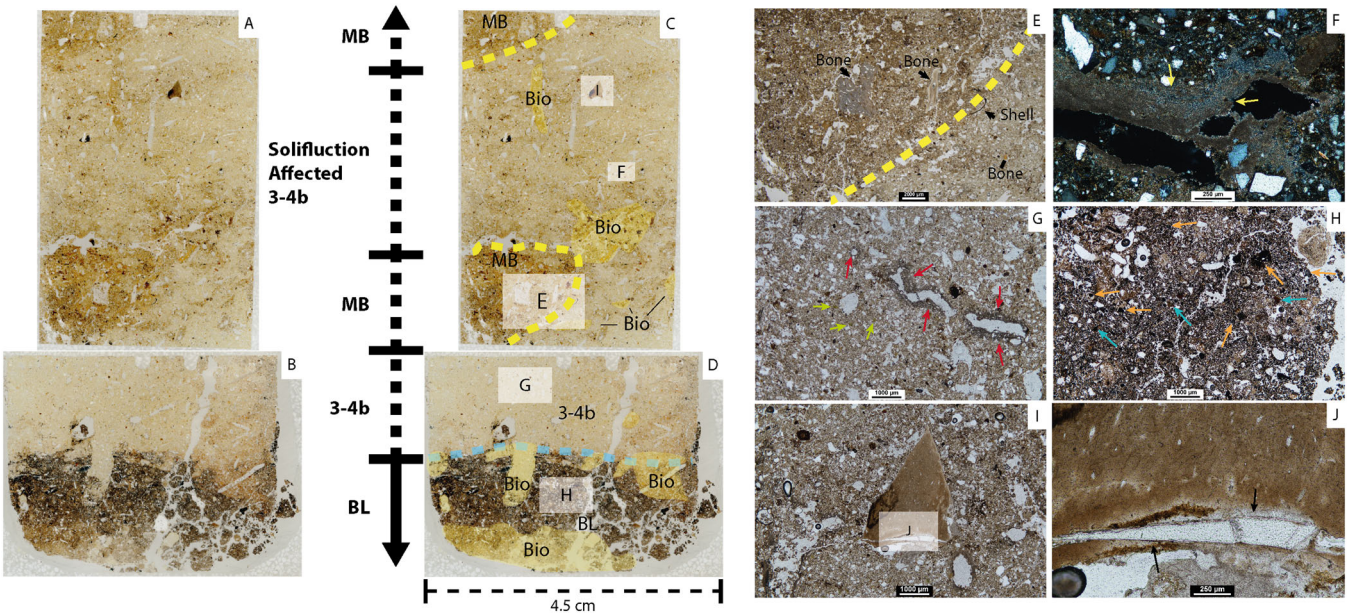

FIGURE 11 | CF1 from AL I in Trench 13-1: Thin sections and photomicrographs from SM-05. (A) and (B) are thin sections scans produced by Spectrum Petrographic. Sections (C) and (D) are the same image with the annotated interfaces between MB and solifluction affected SU 3-4b (yellow line) and MB and BL (light blue line). Bioturbation (Bio) is highlighted in yellow, and the location of the photomicrographs shown below are indicated by the white boxes. (E) Burned (calcined) and unburned bone fragments found near the interface between the MB and solifluction affected SU 3-4b (marked with the yellow line) in PPL, scale is 2000 μm. (F) Secondary calcite (micrite) infilling (marked with yellow arrows) a channel void within the solifluction affected 3-4b, XPL, scale is 250 μm. (G) Complex microstructure of SU 3-4b with few vesicles and channel voids with secondary calcite hypocoating (red arrows) and glauconite grains (light green arrows) PPL, scale is 1000 μm. (H) The BL has a generally spongy microstructure with vughs, vesicles, channel voids throughout the matrix. Sand sized rounded burned organic remains/charcoal (orange arrows), and sand-sized rounded bone fragments (blue arrows) within the BL, PPL, scale is 1000 μm. (I) Lithic fragment embedded within a burned bone, PPL, scale is 1000 μm. (J) Close up of the lithic fragment (black arrows) from (I), PPL, scale is 250 μm.

few voids, as well as domains of very weakly developed lenticular microstructure. This section of SU 4-1b is composed of dense homogenous, well-sorted yellowish-brown silt with few fine sand-sized quartz grains and very fine sand-sized (~100 μm) rounded glauconite grains (Figure 15F). Rhizoliths (root casts) and other secondary carbonate hypocoatings are impregnating the matrix around some of the void spaces. The contact between unburnt SU 4-1b and the overlying RL is relatively sharp but is interrupted by common bioturbation (Figure 15). The RL has a complex microstructure with domains of weakly developed granular and lenticular microstructures. The RL groundmass consists of a dense well-sorted silt with few subangular sand-sized quartz grains (Figure 15E). The contact between the BL and RL (SU 4-1b) is diffused with mixing due to bioturbation commonly found in both deposits (Figure 15). The BL is an organic-rich silt (Figure 15C,D). It has complex microstructure which is generally a massive microstructure punctuated with few chambers, vughs and vermicular structures, as well as domains of very weakly developed lenticular structure. The deposits are composed of very few fine sand/silt-sized unidentifiable burned plant and organic remains (Figure 15C). Above the BL is a thin lens of organically rich silt (MB) of which the organic content increases closer to the BL. In the upper portion of the thin section, there is the solifluction affected loessic sediment with patches of mixed SU 4-1a and 3-4b materials. This layer has a complex microstructure with common chamber voids and few vughs. Unlike the field observations, there is no identifiable ash preserved in the thin sections.

4.3 | Combustion Feature 3

4.3.1 | Macroscopic Descriptions

CF3 is an unlined open flat combustion feature based on the nomenclature proposed by Mallol et al. (2017) (Figure 16). The CF3 structure is located within section 13-B. This structure was uncovered during cleaning of the exposed cliff (section 13-B) and was not fully excavated during the 2013 field season due to time constraints as it would have involved excavating > 2.5 m overlying sediments. CF3 is located in the lower part of SU 4-1b above a thin grey sand horizon (Kulakovska et al. 2021, 235). It is approximately 80 cm in diameter based on the photogrammetry model (Figure 16) using field photos. There is no clear evidence of an ash-rich (white) layer or mottle brown deposits visible from the macro-observations available. The BL is roughly 2–3 cm in maximum thickness, while the RL is approximately 2.6 cm in maximum thickness. There is no clear evidence of stacking or superimposed combustion features (Table 1).

5 | Discussion

Given the lack of in-depth reports on fire use during the LGM (Murphree and Aldeias 2022), it is of interest to better characterize any evidence we have related to combustion behaviours from this period. The combination of both macroscopic and in-depth micromorphological analysis from the site of Korman' 9

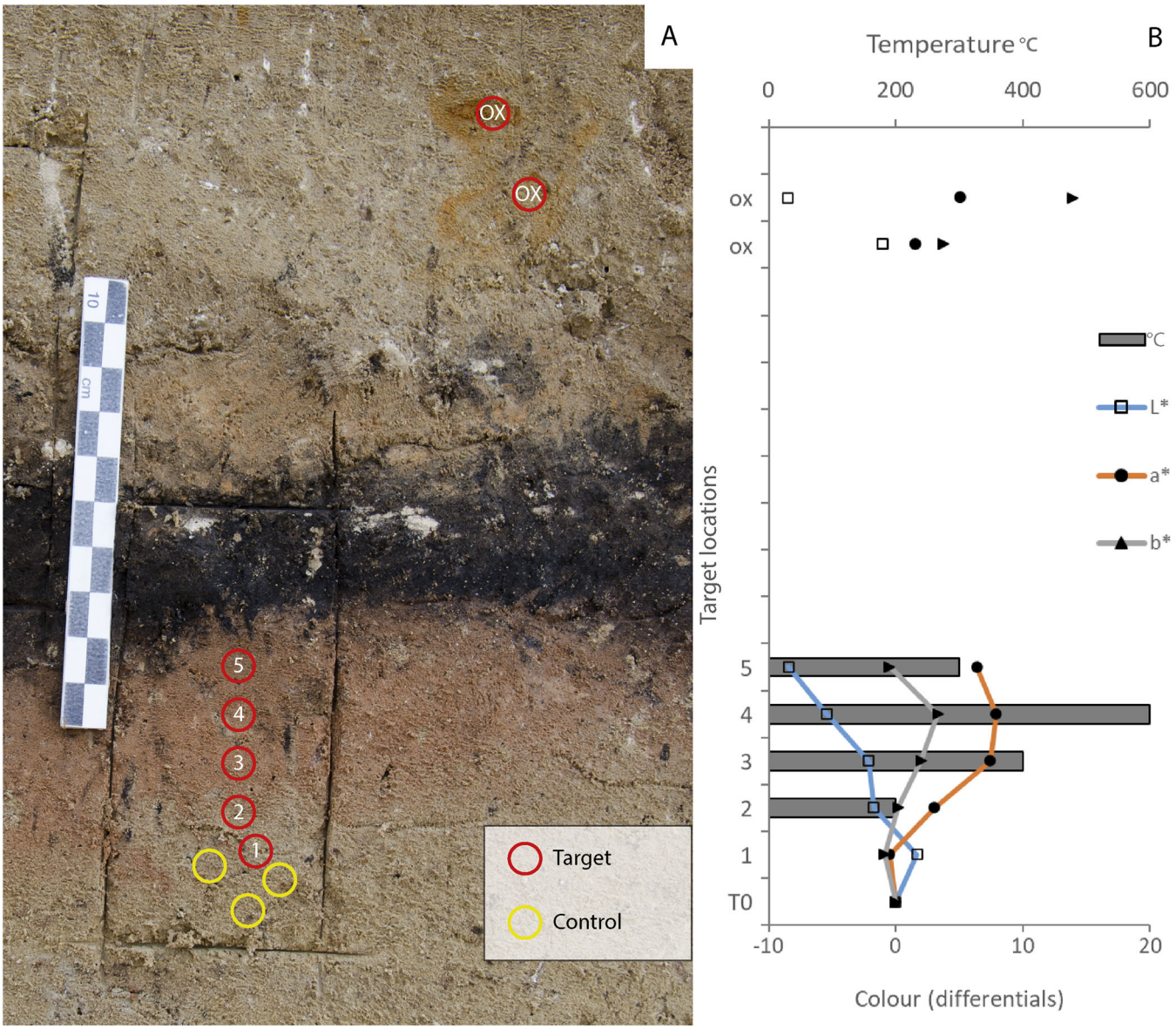

FIGURE 12 | Colorimetric results for CF1. (A) Location of the target (red circles), control (yellow) and oxidized sediments (OX) characterized in the analysis. (B) Colorimetric analysis of the sample locations.

allows us to better characterize the types of features used by Upper Palaeolithic communities at the site, as well as the degree of preservation associated with fire use in open air sites such as Korman' 9. As stated in the section above, CF3 was un-excavated, so our conclusions on site formation and fire related behaviours are limited to the combustion features CF1 and CF2, associated with AL I.

5.1 | CF1: Combustion Residues

Based on the field data and macro-observations, CF1 is an open flat hearth. There is no indication of stone linings or associated features around the combustion feature. The ash component of CF1 is poorly preserved with only isolated domains and small aggregates of recrystallized ash identified in thin section (Figure 9E,F). The plant remains within the BL consist of small organic fragments, some (though not all) of which present some red hues indicative that the materials are not fully combusted. The BL also has some anthropogenic input marked by the presence of isolated ash aggregates, rounded sand-sized burned bone and charcoal fragments. This along with the sharp contact between RL and BL layers and enrichment of the BL with anthropogenic input is likely due to the intensive bioturbation from soil fauna and flora after the abandonment of the feature. This organic-rich composition combined with the considerable thickness and extension of the BL sediments – around 4.4 cm and maximum extent of 1.0 m suggest this layer is a mixture between the burned topsoil of an exposed surface as suggested by Mallol et al. (2013b) and organic remains of non-fully combusted fuels.

There was only one fragment of partially calcined bone visible in an isolated domain of the MB, shown in Figure 11E. Most of the bone fragments found within the BL and MB of CF1 are only partially carbonized (below ~600°C), suggesting the bone

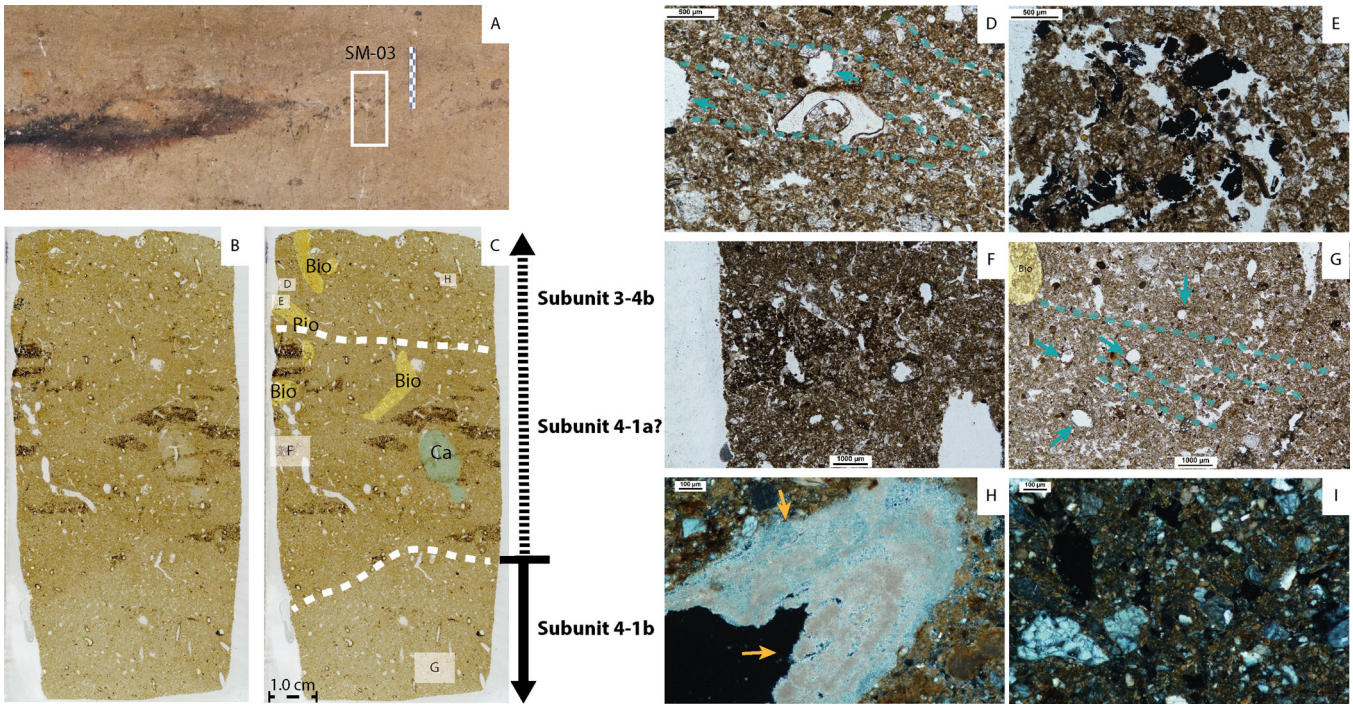

FIGURE 13 | Korman' 9, Trench 13-1: Thin section scans and photomicrographs of SM-03. (A) Orthophotograph of CF1 phase 0, showing the location of SM-03 just to the left of the CF1 deposits. (B) Unaltered thin section scan. (C) Annotated thin section scan of SM-03 with bioturbation (Bio) highlighted in yellow, Calcium carbonate nodule (Ca) shown in blue, and the locations of the photomicrograph indicated by the white boxes. At this sample location SU 4-1a only remains in small bioturbated lenses of sediments, as such it is difficult to delimit the extent of the unit. The diffused tentative limits of SU 4-1a are indicated by the white dashed lines. (D-I) Photomicrographs from SM-03. (D) Photomicrograph of unburned bone fragment found within SU 3-4b; PPL scale is 500 μm. SU 4-1a has a weakly developed laminar structure (light blue lines) and vesicles (blue arrow). (E) Burned organic materials within a bioturbated section of SU 3-4b, PPL scale is 1000 μm. (F) Bioturbated organic silt rich lens of SU 4-1a, PPL scale is 1000 μm. The lenses are more clay rich than the surrounding sediment of SU 3-4b, shown in photomicrograph (I), XPL scale is 100 μm. (G) Weakly developed lenticular microstructure (light blue line) with vesicles (blue arrows) within SU 4-1b, PPL, scale is 1000 μm. SU 4-1b in this sample has complex microstructure, which is generally very dense and massive within the upper section of the sample then becomes more granular and platy nearer the base of the sample. In this photomicrograph, the microstructure is weakly developed laminar/platy with frequent vesicles, channels and vughs likely derived from freeze-thaw processes. (H) Thick micritic infilling (orange arrows) of a channel void within SU 3-4b, XPL scale is 1000 μm. (I) Close up view of the clay rich matrix of the organic lenses (SU 4-1a) from within Figure 13F, XPL, scale is 100 μm.

fragments were not directly exposed to high temperatures associated with a flaming fire (Stiner et al. 1995) (See also: Bosch et al. 2024; Bosch et al. 2012; Gallo et al. 2021; Théry-Parisot 2002; Théry-Parisot et al. 2005). However, it is possible that the presence of unidentified burned organic remains (potentially char or burned animal fats) within the MB and mixed within the BL of CF1 is due to subsistence practices (Bosch et al. 2024). Based on our observations of lack of calcined spongy bone and common charcoal fragments, we can conclude that wood, not bone is the primary fuel source for CF1. Although we cannot exclude the use of dung or fats as fuels at this stage of analysis. The scarcity of larger charcoal fragments within the thin sections makes it difficult to determine which type of wood was the primary fuel source, though the anthracological analysis of the available macroscopic charcoal collected from excavations to date points to a predominance of *Picea* (Kulakovska et al. 2021).

In terms of post-depositional processes, CF1 shows clear macroscopic evidence of solifluction with stretching and overthrow of the BL, visible in Figure 6B,C. Within the micromorphological thin sections of CF1, the presence of weakly developed lenticular and domains of granular microstructures within the red layer (SU 4-1b) gives credence to freeze-thaw related post-depositional alteration in the underlying SU 4-1b (Van Vliet-Lanoë 1985, 2010) (Figures 8–1 and 9). This includes discrete evidence of inverse grading, commonly seen in collapsed lenticular structures, and, within the upper combustion deposits, BL and MB, some of the charcoal fragments appear cracked by frost action (Matthiesen et al. 2013). Cappings are also visible on some aggregates within the MB deposit (Figure 7E) (Van Vliet-Lanoë 1985, 2010). However, due to the extensive bioturbation within the sampled sections, it is difficult to ascertain the extent of cryoturbation within the CF1 deposits at a microscopic scale.

The results of the colorimetric analysis of CF1 appear consistent to temperatures for wood-fuelled combustion features. Wood fire features can potentially achieve maximum temperatures above 950°C depending on several different factors (e.g., fuel type, amount of fuel, moisture content, conditions of the underlying substrate) (Aldeias et al. 2016; Bentsen 2013; Hoare 2020). High surface temperature then transfers heat down into the underlying substrate, and our results of temperatures reaching 600°C in the subsurface, redden RL layer, of CF1 are relatively consistent with those from experiments by Aldeias

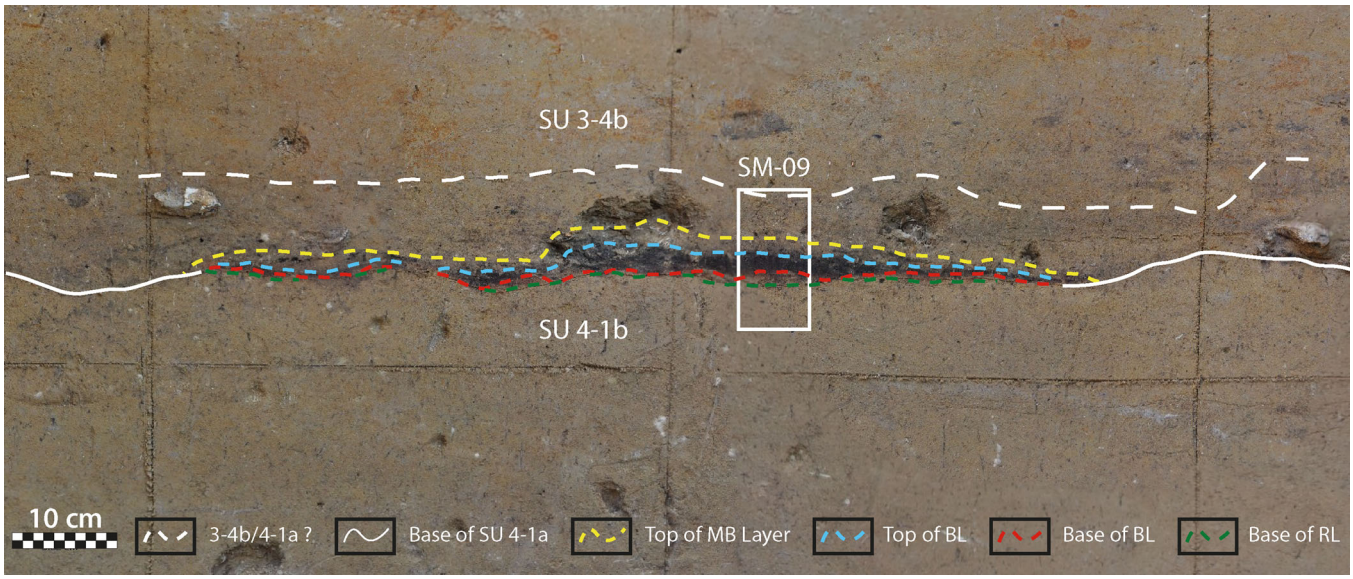

FIGURE 14 | Korman' 9, Trench 13-2, AL I, CF2: Orthophotograph of the CF2. The white boxes show the location for soil micromorphology sample (SM-09). The four lines indicate the different interfaces between the combustion feature deposits: yellow = top of the MB deposit, light blue = the top of the BL, red = the base of the BL, and the green indicates the base of the RL. The solid white line delimits the contact between SU 4-1a and 4-1b. The dashed white line indicates the upper contact between 4-1a and 3-4b which is unclear with potentially several instances of solifluction and overlapping deposits. The boundaries between the two SUs are diffused with mixing throughout.

et al. (2016, 73). The diffused character of the BL and RL of CF2 made temperature estimation using the method above non-viable.

5.2 | CF2: Combustion Residues

CF2 is also an open flat hearth structure with no evidence of a stone lining or secondary features around it. Based on the sampled area of CF2, there were no preserved ash domains or lenses. The BL in CF2 is only partially preserved within the sampled section (Figure 15) with a diffused boundary between the BL and RL deposits. In stark contrast to the BL of CF1, CF2 is nearly devoid of identifiable burned plant remains, with much of the very few organic materials appearing as amorphous black nodules under the microscope. Based on our micro-observations, the BL of CF2 is considerably less dense in organic materials than the BL of CF1. Additionally, SM-09 has no burned bone fragments within either the MB or BL deposits. The microstructure of underlying SU 4-1b, the combustion deposits and overlying SU 3-4b within SM-09 have weakly developed pedality and separation between the sedimentary materials (Stoops 2003) meaning the microstructure is generally massive. The only evidence of cryoturbation is isolated lens of preserved capping, vesicles and domains of weakly developed lenticular microstructure within the RL (4-1b) and BL shown in Figure 15.

Overall, the general lack of well-preserved ash layers, combined with the fragmented nature of the bone and charcoal, suggest that both CF1 and CF2 were exposed on the surface for a prolonged period. Conditions with high wind or run off would favour the erosion of the ashes, whereas we do not see signs of dissolution and reprecipitation of the remaining ash domains. This conclusion of a stasis from deposition and exposure of the occupation surfaces is supported by extensive aerial weathering and in situ fragmentation of faunal remains from Korman' 9 as described by Kulakovska et al. (2021) and Bosch et al. (2024).

5.3 | Anthropogenic Soils and Bioturbation

The influx of organic waste and materials by humans can have a knock-on effect in terms of promoting soil fauna activity and biodiversity in the subsequent deposits (Schilt et al. 2017). At Korman' 9, the BL and MB of both features have extensive post-depositional bioturbation and pedogenesis as shown in Figures 7, 10, and 11, similar to those reported by Schilt et al. (2017) at the Late Gravettian site of Grub-Kranawetberg I (Austria). The MB deposit of CF1 and CF2 developed after use of the combustion feature and is likely the result of localized gradual mixing of loessic materials (potentially SU 3-4b) with the organic- rich materials left from anthropogenic occupations, including fire use. In the MB deposit from CF1, there is clear evidence of carbonate enrichment with the formation of cm-sized carbonate nodules as well as micritic hypocoating and root casts, whereas the MB deposits associated with CF2 are less developed in comparison. Similarly, the BL of CF2 is less rich in organic matter and charred materials than the BL associated with CF1. This could suggest that either the topsoil below CF2 was less carbonized due to burning for a shorter period than CF1 or contained less organic material syn-combustion. The latter possibility is further discussed in the section below. In contrast to the micromorphological samples from the combustion features, SM-03, taken approximately 30 cm laterally from CF1 during the initial stages (Phase 0) of excavation (Figure 6), shows only limited lenses and domains of organic-rich silts which appear to be the remnants of SU 4-1a (Figure 16).

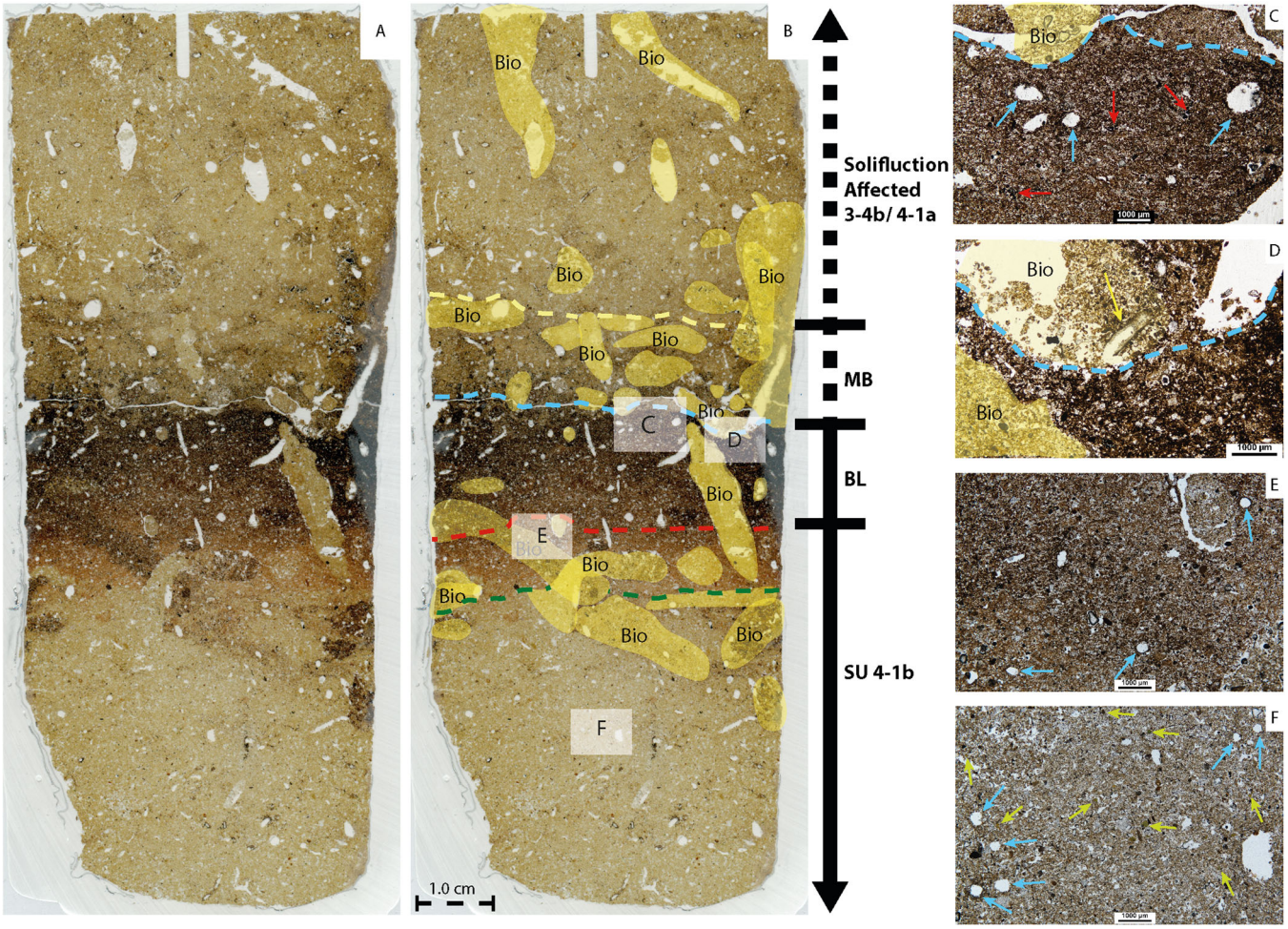

FIGURE 15 | Korman' 9, Trench 13-2, AL I, CF2: SM-09 thin sections and photomicrographs. (A) thin section scan of SM-09. (B) thin section scan of SM-09 with the annotated interfaces between the solifluction affected SU 3-4b/4-1a deposit and top of MB (yellow line), top of BL (blue line) and top RL (red line) and contact between the base of RL (burned 4-1b) and unburned SU 4-1b (green line). Bioturbation (Bio) are highlighted in yellow. Photomicrograph locations are shown in the white boxes. (C) Photomicrograph of dark organic BL sediments with vesicles (blue arrows). Burned plant remains are very rare within the BL, some of which are indicated by the red arrows. (D) Root cast (yellow arrow) found at the interface of the BL and MB, PPL scale is 1000 µm. Yellow shaded regions indicate bioturbation. (E) Dispersed organic matter mixing within the RL, PPL, scale is 1000 µm. The RL microstructure is generally well-sorted, massive with very few vesicles (blue arrows) and channels (due to bioturbation). (F) unburned SU 4-1b underneath CF2, PPL, scale is 1000 µm. SU 4-1b has a massive microstructure with some vughs, vesicles (blue arrows) and rare vermicular structures resulting from the burrowing of soil microfauna. It also has common fine sand size glauconite (greenish yellow arrows) and quartz grains.

5.4 | Fire Use at Korman' 9

Based on the morphological and compositional variation between CF1 and CF2 (including the dimensions, thickness and nature of the combustion deposits, presence and nature of post-depositional alternations), we can suggest two different explanations. The differences between CF1 and CF2 could (1) represent two distinct occupations or (2) a single occupation with variations due to patterns in site organization and/or differences in function. The current archaeological evidence available for this study, including high resolution lithic and fauna analysis, is described in detail by Bosch et al. (2024) and Kulakovska et al. (2021) and does not support or negate either interpretation. Further studies that could aid our interpretations, such as refitting analysis, are on-going and not available for this study.

If we consider the first hypothesis, then CF1 and CF2 would represent two distinct occupations within the same stratigraphic SU 4-1a. We currently lack the resolution to temporally confine CF1 and CF2 to create a clear time frame between the occupations and accumulations or to attest to their contemporality. The usage of CF1 and CF2 could be separated by a matter of weeks to centuries. However, we can suggest contrasts between the BL deposits of CF1 and CF2, and the distinct development of the degree of cryoturbation sedimentary signatures could indicate different depositional times between the two features. First, the distinction between the presence of organics within the BL of CF1 and CF2 could potentially be product of several factors. One of which could be related to seasonality with the firing of CF1 corresponding to season (fall) where more organic litter maybe present on the surface and topsoil, while CF2 could have been fired during late spring or summer where organic litter is not present in the topsoil. Conversely, the occupations could be separated by some time, resulting in different conditions for the presence of organics in the topsoil. Second, based on our observations, we can identify a

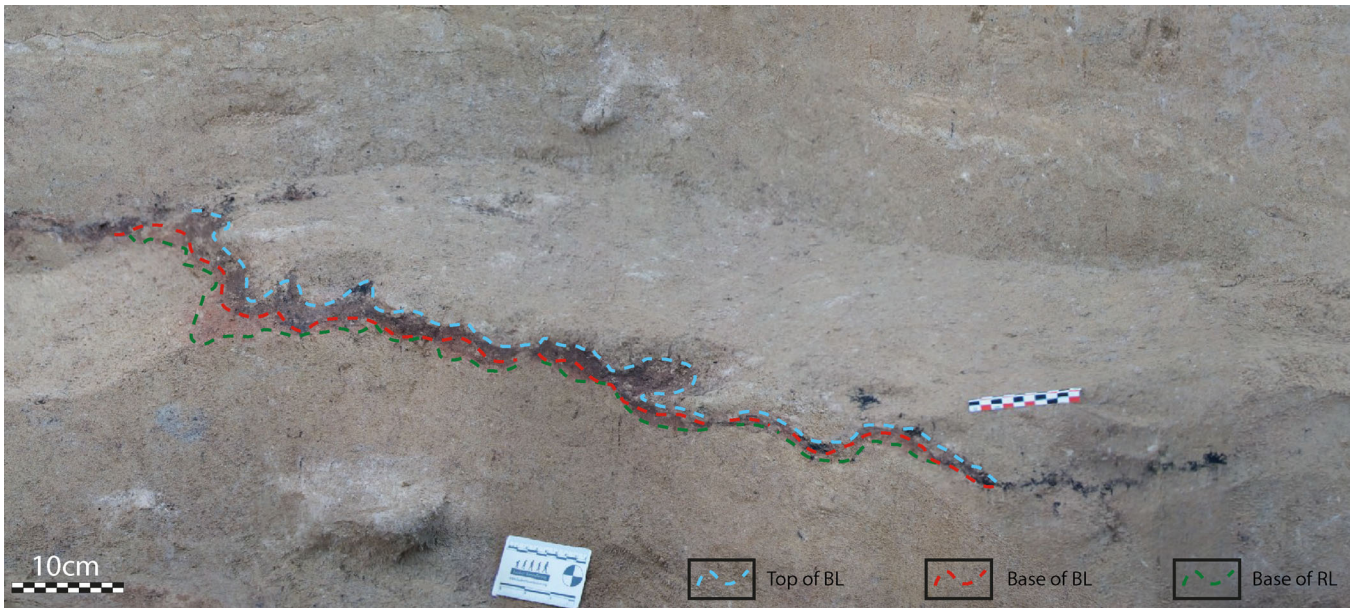

FIGURE 16 | Korman' 9, Section 13-B, AL II, CF3: View of the CF3 based on the model produced in Agisoft Metashape. The dashed lines indicate the various limits between the layers of CF3. The three lines indicate the different interfaces between the deposits of the combustion feature: light blue = the top of the BL, red = the base of the BL, and the green indicates the base of the RL. Model credit: W.C. Murphree.

distinct difference between the nature of cryoturbation related to CF1 and CF2. CF1 appears to have more clear evidence of post-depositional alteration with development of lenticular and granular structures (albeit weakly developed) within thermally altered deposits as well as surrounding substrate. While we are limited to only a single sample for CF2 (SM-09), the effects of cryoturbation are less clearly visible or well preserved on a microscopic scale. Moreover, as discussed in the section above, CF2 has weakly developed pedality and nearly no separations between peds in the sedimentary matrix. This suggests the deposition of CF2 could have taken place in slightly different environmental conditions.

Considering the second hypothesis mentioned above, CF1 and CF2 could represent the same occupation but vary morphologically based on site organization. Based on the dimensions and morphology of the CF1 structure, including the much thicker RL and BL layers (Figure 6), we can assume CF1 was used more intensely than CF2. Using the morphology (namely the thickness) of the RL, it can be argued CF1 was either fired during a longer period and/or the fire was maintained at a higher temperature than CF2. As shown in experimental studies, the most significant thermal alteration of the underlying sediment takes place over the first 2–3 h of burning (Aldeias et al. 2016). Moreover, the depth of rubification varies depending on the substate, the presence of thermal insulators on the burning surface, as well as the duration and intensity of the fire use (Aldeias et al. 2016). This evidence suggests that CF1 could have been used for a prolonged period and/or fired at a higher temperature. Therefore, the variations between the two structures could be associated with site organization and settlement strategies (Binford 1978; Binford 1980; Clark et al. 2022; Rolland 2018; Stapert 1989). In a similar vein, the differences between CF1 and CF2 could be due to function. While, the function of combustion features is often unclear (Aldeias 2017; Aldeias et al. 2016), the variations of organic input could be the result of repeated refuelling of CF1 compared to CF2. The differences between the effects of cryoturbation could be localized due to several factors, such as localized drainage conditions, presence of surface matter, snow cover, etc. It is possible that the post-depositional effects of cryoturbation could represent a mosaic of different localized conditions rather than multiple events converging over time. Again, due to the extensive bioturbation in both CF1 and CF2, our conclusions should be treated with a grain of salt and future analysis and more sampling across SUs 3-4b, 4-1b and 4-1a can provide more insights into the topography of these palaeosurfaces, as well as the nature of post-depositional processes at the site.

Regardless of timing of the occupations, after the combustion features were used, the site was likely abandoned. The lack of ash and the fragmentary nature of the charcoal remains within CF1 and CF2 implies that the occupational debris of AL I were exposed to the elements over some time. Both combustion features were also intensively bioturbated by soil microfauna and localized plant growth. Overall, the absence of evidence for stacking or superimposed combustion features at the site, combined with the evidence of long-term exposure of the combustion residues, suggest that these features were not reutilized after their initial abandonment. Several ethnographic studies have shown human hunter-gatherer groups tend to reuse the same location for lighting combustion features (Mallol and Henry 2017; Mallol et al. 2007; McCauley et al. 2020). This suggest that, if CF1 and CF2 were separate occupations, then it is likely that the timing for each of occupations was separated for a long enough period time that the initial occupation area was already buried from view. Vice versa, if they are from the same occupation then, the site was not re-occupied within the excavated portions of AL I. After the abandonment, the evidence for solifluction processes, as described by Kulakovska et al. (2021) and Bosch et al. (2024), suggests gradual movements of parts of the combustion features and other materials (shown in Figure 6) downslope.

TABLE 1 | Micromorphological sample ID and general micromorphological descriptions based on Stoops (2003).

Sample ID	Feature	Stratigraphic subunit (SU)	C/F distribution	b-Fabric	Microstructure (MS)	Groundmass and pedofeatures	Components
SM−01	CF1	3-4b	Open-Porphyric	3-4b—Calcitic crystallitic and mosaic.	3-4b—Generally massive with weakly developed platy structure.	3-4b—Homogenous dense well sorted silt with common subangular fine sand-sized quartz grains, calcite rich groundmass, frequent secondary calcific hypocoatings and rhizoliths.	3-4b—Few rounded glauconite, small cm-sized carbonate nodules, muscovite, and subangular shell fragments.
		Brown mottled layer (MB)	Open-Porphyric	MB—Calcitic crystallitic and mosaic.	MB—Vughy with some domains of vermicular and weakly developed lenticular MS.	MB—Well sorted silt with common fine sand sized quartz, some organics, clear channels and bio galleries from soil fauna/flora, presence of cm-sized carbonate concretions, and capping present on few aggregates.	MB—Few 1 mm sized rounded clay aggregates, muscovite, and frequent burned plant remains (associated with bioturbation).
		Black layer (BL)	Open-Porphyric	BL—Undifferentiated	BL—Vughy/spongy MS	BL—Dense, organic-rich silts with common fine sand size quartz grains, densely bioturbated with abundant channels and vermicular structures.	BL—Very dominant burned and partially burned plant remains, burned organic remains, and very few partially burned bone (stage 2 and 3).
SM-02	CF1	BL	Open-Porphyric	BL- Undifferentiated	BL- Vughy/spongy MS.	BL—Dense organic-rich silt with common fine sand-size quartz grains, densely bioturbated with abundant channels and vermicular structures.	BL—Very dominant burned and partially burned plant remains, burned organic remains, and rare partially burned bone (stage 2 and 3), and very few fragments of ash lenses.
		4-1b-Red Layer (RL)	Open-Porphyric	RL—Generally calcitic crystallitic and	RL—Weaky developed lenticular/granular.	RL—Thermally altered dense well sorted silt	RL—Few partially burned plant remains

(Continues)

TABLE 1 | (Continued)

Sample ID	Feature	Stratigraphic subunit (SU)	C/F distribution	b-Fabric	Microstructure (MS)	Groundmass and pedofeatures	Components
				mosaic with domains of granostriated.		with common fine sand size quartz.	derived from bioturbation, very few thermally altered glauconite, and few secondary carbonates infilling of void spaces.
		4-1b	Open-Porphyric	4-1b-Calcitic crystallitic	4-1b—Generally massive with domains of weakly developed platy/granular MS near RL interface.	4-1b—Homogenous dense well sorted silt with common subangular fine sand sized quartz grains, and capping present on some aggregates.	4-1b—Few glauconite grains, rhizoliths, and secondary $CaCO_3$ infilling.
SM-04	CF1	MB	Open-Porphyric	MB-Speckled and calcitic crystallitic.	MB—Generally massive MS.	MB—Well sorted silt with common fine sand sized quartz, some organics, clear channels and bio galleries from soil fauna/flora, with a diffused interface with 3-4b.	MB—Few rounded glauconite, small cm sized carbonate nodules, few unburned bone fragments very few silex fragments, antler fragment, rhizoliths and secondary $CaCO_3$ infilling.
		BL	Open-Porphyric	BL—Undifferentiated	BL—Vughy/spongy MS	BL—Dense organic-rich silt with common fine sand-size quartz grains, densely bioturbated with abundant channels and vermicular structures.	BL—Dominant burned and partially burned plant remains.
		4-1b	Open-Porphyric	4-1b—Speckled and calcitic crystallitic.	4-1b—Generally massive MS.	4-1b—Homogenous dense well sorted silt with common fine sand sized subangular quartz grains, few vughs without hypocoatings.	4-1b—Few rounded glauconite, small cm sized carbonate nodules, muscovite, few subangular shell fragments; very few silex fragments.

(Continues)

TABLE 1 | (Continued)

Sample ID	Feature	Stratigraphic subunit (SU)	C/F distribution	b-Fabric	Microstructure (MS)	Groundmass and pedofeatures	Components
SM-05	CF1	Solifluction affected 3-4b	Open-Porphyric	3-4b—Speckled and calcitic crystallitic	3-4b—Complex MS	3-4b—Mottled, dense, well sorted silt with common fine sand sized subangular quartz grains, some vughs w/o hypocoatings, 3-4b becomes more homogenous closer to BL layer.	3-4b—Few glauconite grains, rhizoliths, secondary $CaCO_3$ infilling, bone fragment with embedded silex, and rare charcoal fragment.
		MB	Open-Porphyric	MB—Speckled and calcitic crystallitic.	MB—Complex MS	MB—Well sorted silt with common fine sand sized quartz, and some organics.	MB—Few rounded glauconite, small cm sized carbonate nodules, and few unburned bone fragments.
		BL	Open-Porphyric	BL—Undifferentiated	BL—Vughy/spongy MS	BL—Organic- rich silt with common fine sand size quartz grains, densely bioturbated with common channels and vermicular structures.	BL—Dominant burned and partially burned plant remains
SM-09	CF2	Solifluction affected 3-4b/ 4-1a	Open-Porphyric	3-4b—Speckled	3-4b—Massive MS with domains of very weakly developed lenticular MS.	3-4b—Mottled, dense, well sorted silt with common fine sand size quartz grains, calcite rich.	3-4b—Few glauconite grains, rhizoliths, secondary $CaCO_3$ infilling.
		MB	Open-Porphyric	MB—Speckled	MB—Generally massive MS	MB—Well sorted silt with common fine sand sized quartz, some organics, bioturbated with mixing of material from underlying BL.	MB—Rare burned and partially burned plant remains.
		BL	Open-Porphyric	BL—Undifferentiated	BL—Generally massive with domains of weakly developed lenticular MS	BL—Dense organic-rich silt, densely bioturbated.	BL—Very few burned and partially burned plant remains.

(Continues)

TABLE 1 | (Continued)

Sample ID	Feature	Stratigraphic subunit (SU)	C/F distribution	b-Fabric	Microstructure (MS)	Groundmass and pedofeatures	Components
		4-1b- RL	Open-Porphyric	RL—Undifferentiated	RL—Generally massive MS with domains of very weakly developed lenticular MS.	RL—Thermally altered, dense well sorted silt with common fine sand-size quartz grains	RL—Very few partially burned plant remains derived from bioturbation, very few thermally altered glauconite, few secondary carbonate infilling of void spaces.
		4-1b	Open-Porphyric	4-1b—Speckled	4-1b—Generally massive MS with domains of very weakly developed lenticular MS.	4-1b—Homogenous, dense, well sorted silt with common fine sand size quartz grains, calcite rich.	4-1b—Few rounded glauconite, very few shell fragments, and very few burned plant remains.
SM-03	Control sample about 30 cm west of CF1	3-4b	Open-Porphyric	3-4b—Speckled clays and calcitic crystallitic	3-4b—Complex MS. Granulated MS at the base with a more massive MS towards the upper portion of the section, domains of lenticular MS.	3-4b—Dense well sorted silt with common fine sand sized quartz, some lenses of more organic silt (4-1a).	3-4b—Few glauconite grains, rhizoliths, secondary $CaCO_3$ infilling, and very few sand sized bone fragments
		4-1b	Open-Porphyric	4-1b—Speckled clays and calcitic crystallitic.	4-1b—Generally massive MS with some domains of weakly developed lenticular MS.	4-1b—Homogenous, dense well sorted silt with common fine sand sized quartz.	4-1b—Few glauconite grains, rhizoliths, and secondary $CaCO_3$ infilling.

5.5 | Korman′ 9 in Context

Similar combustion structures to CF1 and CF2 have been found in nearby sites in the Middle Dniester region. Several of which have occupations occurring during a similar period of the LGM as Korman′ 9. These include the nearby sites of Korman′ IV, Molodova V and Doroshivtsi III (Haesaerts et al. 2007; Haesaerts et al. 2003; Kulakovska et al. 2015; Noiret 2009; Noiret et al. 2021). While the combustion features at these sites are not described in detail, their presence is usually associated with potential hut-like structures or concentrations of lithic artefacts and faunal remains (sometimes interpreted as activity areas) (Chernysh 1977, 1987; Klein 1973; Kulakovska et al. 2015; Murphree and Aldeias 2022; Noiret 2009). The sites of Korman′ IV (Layer 5a) and Molodova V (Layer 6) feature dozens of combustion features directly associated with combustion structures or hearths and activity areas (Chernysh 1977, 1987; Noiret 2009). Some of which, such as those associated with Layer 5a at Korman′ IV, are potentially lined with limestone slabs (Noiret 2009). Other combustion features, such as those from Layer 6 of Molodova V, have nearby secondary pit features and individual charcoal lenses that could be related to combustion feature maintenance (Chernysh 1987; Noiret 2009). Two fireplaces were found in Doroshivtsi III, Level 3, and are tentatively associated with Late Gravettian materials (Kulakovska et al. 2015). However, the lack of well- described reports on the nature and components of the combustion features at these sites means that implications for understanding fire use in the Middle Dniester region remains limited (Murphree and Aldeias 2022).

When comparing the combustion features of Korman′ 9 on a larger regional scale, it can be inferred that open flat combustion features generally dominate the late and post-LGM landscape (Chabai et al. 2022; Murphree and Aldeias 2022). Flat combustion structures have been recently described at the Ukrainian Epigravettian site of Barmaky (Chabai et al. 2022). The authors describe a flat, unlined combustion feature, roughly 1.36×0.71 m dimensionally and 0.08 m thick, though it is unclear if there is a thermally altered red layer associated with the structure (Chabai et al. 2022, 116). Several fireplaces were also documented in layers 5 and 4 at the Moldovan site of Cosautşi, located further south on the Dniester River; although it is unclear based on their description, what their morphology is (Noiret 2004, 2009). Other types of features have been described at the sites of Mezhyrich (Ukraine) with potential evidence of pit combustion features (Marquer et al. 2015; Marquer et al. 2012). However, none of the combustion features at Mezhyrich have been described in detail, hampering regional comparisons on pyrotechnology.

The combustion features Korman'9 are amongst the first high-resolution descriptions of fire use in Europe during the LGM. The use of simple flat combustion structures at this site could represent a significant change in behaviour, in terms of resource management and social organization, compared to earlier periods of the Upper Palaeolithic (Murphree and Aldeias 2022). As fire use is a costly and resource-intensive behaviour (Henry 2017; Henry et al. 2018), limiting the investment in the structural complexity of combustion features could be interpreted as a response to increasingly unfavourable environmental conditions and resource stress in various groups and populations. This is not to say that the fire use behaviours at Korman'9 are representative for all modern human fire use during the LGM. However, there is a clear bias in terms of the publication of combustion feature descriptions during this period that needs to be further addressed. Additionally, we also currently lack intensive studies looking at the preservation of combustion features in periglacial conditions. As we have shown through the results and discussion, the combustion features in AL I have been affected to various extents by biogenic and geogenic processes including cryoturbation. The extent of which the process disrupt and influence the interpretation of fire use and structures in glacial periods needs to be addressed before drawing more generalized conclusions. Overall, we need more detailed studies of LGM fire use to better understand how modern human populations were able to employ fire use as a tool, its structural variability and its preservation in the archaeological record.

6 | Concluding Remarks

Here, we have presented the results of our geoarchaeological study of the combustion features of the LGM site of Korman′ 9. Our study represents the first detailed micromorphological descriptions of combustion features during the height of the LGM for this region. All of the combustion features identified at Korman'9 can be described as open flat hearths. Based on our results, we can infer that CF1 was a wood fuelled, open flat combustion feature. The lack of a clear ash layer and the highly fragmented nature of the charcoal and bone fragments within the combustion feature suggest that the feature was exposed on the surface for a prolonged period. However, new data sets are needed to better understand how exposure of combustion remains during glacial periods affects the preservation of ashes and other fire residues. CF2, on the other hand, is a smaller open flat hearth with limited remaining organic materials. Additionally, it is clear from our field observations, 3D models and descriptions that both combustion features were post-depositionally altered by cryoturbation and bioturbation. As a result, we can suggest several explanations for the differences between the two combustion features: (1) two separate occupations separated by an unknown period, yet within the same stratigraphic subunit or (2) same occupation but differentiated by site organization and/or function. In comparison with the limited evidence from the Middle Dniester region, open flat hearths appear to have been the primary form of pyrotechnology created by humans during the LGM. The presence of structurally more complex features (with pit and stone-lined hearths) is alluded for some sites (Mezhyrich and Korman′ IV) and further research into the nature and composition of these features is needed to provide a more holistic view on the use of fire during extreme cold periods (Chernysh 1977; Marquer et al. 2012; Noiret 2004, 2009). Overall, more research and detailed macro- and micromorphological studies are needed to better understand the relationship between combustion features and the spatial organization of human occupations in the region. Future experimental studies should also focus on better constraining the effects of cryo-related processes on the preservation of combustion residues. In conclusion, our results provide new insights into human fire use behaviour at the height of the LGM and highlight new avenue of research for future studies in the region and beyond.

Acknowledgments

The authors would like to thank Carolina Mallol, Paul Goldberg, Hans Huisman and Pierre Noiret for their support and advice. This research was funded in part by the Fundação para a Ciência e a Tecnologia, I.P. (FCT, https://ror.org/00snfqn5816) under Grant (UID/04211: Centro Interdisciplinar de Arqueologia e Evolução do Comportamento Humano (ICArEHB), as well as FCT grant numbers 2021.08939.BD (to WCM) and PTDC/HAR ARQ/29606/2017 (to VA). For the purpose of Open Access, the author has applied a CC-BY public copyright license to any Author's Accepted Manuscript (AAM) version arising from this submission. Further support was provided by the European Research Council (ERC) MATRIX Project 101041245 (to VA). The fieldwork and analysis were funded by the following grants to PRN: EC FP7 Marie Curie Career Integration Grant no. 322261 (NEMO-ADAP Project), Leakey Foundation General Grant (spring 2012 granting cycle), D.M. McDonald Grants and Awards Fund grants, Isaac Newton Trust Small Grant, Isaac Newton Trust Matching Funding Grant, British Academy/Leverhulme Trust Small Grant, and funds of the Max-Planck-Society. M.D.B. was supported through an EC H2020 MSCA Grant (grant no. 656325, EU-Beads project) and a Seal-of-Excellence-Fellowship (TechnoBeads project) of the Austrian Academy of Sciences. V.I.U. was supported by the Researchers at Risk Fellowship of the Czech Academy of Sciences.

Ethics Statement

This research did not involve human participants and/or animals.

Conflicts of Interest

The authors declare no conflicts of interest.

References

Agisoft. 2021. "Agisoft Metashape Professional (Version 1.75)."

Aiello, L. C., and P. Wheeler. 1995. "The Expensive-Tissue Hypothesis: The Brain and the Digestive System in Human and Primate Evolution." *Current Anthropology* 36, no. 2: 199–221.

Aldeias, V. 2017. "Experimental Approaches to Archaeological Fire Features and Their Behavioral Relevance." *Current Anthropology* 58, no. S16: S191–S205.

Aldeias, V., H. L. Dibble, D. Sandgathe, P. Goldberg, and S. J. P. McPherron. 2016. "How Heat Alters Underlying Deposits and Implications for Archaeological Fire Features: A Controlled Experiment." *Journal of Archaeological Science* 67: 64–79. https://doi.org/10.1016/j.jas.2016.01.016.

Anghelinu, M., M. Händel, L. Niță, et al. 2020. "From Gravettian to Epigravettian in the Eastern Carpathians: Insights From the Bistricioara-Lutărie III Archaeological Site." *Quaternary International* 587–588: 210–229. https://doi.org/10.1016/j.quaint.2020.06.044.

Aydemir, S., S. Keskin, and L. R. Drees. 2004. "Quantification of Soil Features Using Digital Image Processing (DIP) Techniques." *Geoderma* 119, no. 1–2: 1–8.

Banks, W. E., F. d'Errico, A. T. Peterson, et al. 2008. "Human Ecological Niches and Ranges During the LGM in Europe Derived From an Application of Eco-Cultural Niche Modeling." *Journal of Archaeological Science* 35, no. 2: 481–491. https://doi.org/10.1016/j.jas.2007.05.011.

Bentsen, S. E. 2013. "Controlling the Heat: An Experimental Approach to Middle Stone Age Pyrotechnology." *South African Archaeological Bulletin* 68, no. 198: 137–145.

Beresford-Jones, D., S. Taylor, C. Paine, A. Pryor, J. Svoboda, and M. Jones. 2011. "Rapid Climate Change in the Upper Palaeolithic: The Record of Charcoal Conifer Rings From the Gravettian Site of Dolní Věstonice, Czech Republic." *Quaternary Science Reviews* 30, no. 15–16: 1948–1964. https://doi.org/10.1016/j.quascirev.2011.04.021.

Beresford-Jones, D. G., K. Johnson, A. G. Pullen, A. J. E. Pryor, J. Svoboda, and M. K. Jones. 2010. "Burning Wood or Burning Bone? A Reconsideration of Flotation Evidence From Upper Palaeolithic (Gravettian) Sites in the Moravian Corridor." *Journal of Archaeological Science* 37, no. 11: 2799–2811. https://doi.org/10.1016/j.jas.2010.06.014.

Binford, L. R. 1978. *Nunamiut Ethnoarchaeology*. New York: Academic Press New York.

Binford, L. R. 1980. "Willow Smoke and Dogs' Tails: Hunter-Gatherer Settlement Systems and Archaeological Site Formation." *American Antiquity* 45, no. 1: 4–20.

Bosch, M., L. Kulakovska, V. Usyk, O. Kononenko, P. Spry-Marqüis, and P. Nigst. 2024. "Human-Animal Interactions at Korman'9 Ukraine." *Archaeology and Early History of Ukraine* 50, no. 1: 119–138.

Bosch, M. D., P. R. Nigst, F. A. Fladerer, and W. Antl-Weiser. 2012. "Humans, Bones and Fire: Zooarchaeological, Taphonomic, and Spatial Analyses of a Gravettian Mammoth Bone Accumulation at Grub-Kranawetberg (Austria)." *Quaternary International* 252: 109–121. https://doi.org/10.1016/j.quaint.2011.08.019.

Braadbaart, F., I. Poole, H. D. J. Huisman, and B. van Os. 2012. "Fuel, Fire and Heat: An Experimental Approach to Highlight the Potential of Studying Ash and Char Remains From Archaeological Contexts." *Journal of Archaeological Science* 39, no. 4: 836–847. https://doi.org/10.1016/j.jas.2011.10.009.

Canti, M. G. 2003. "Aspects of the Chemical and Microscopic Characteristics of Plant Ashes Found in Archaeological Soils." *Catena* 54, no. 3: 339–361. https://doi.org/10.1016/s0341-8162(03)00127-9.

Canti, M. G., and N. Linford. 2000. "The Effects of Fire on Archaeological Soils and Sediments: Temperature and Colour Relationships." Paper presented at the Proceedings of the Prehistoric Society.

Chabai, V., D. Dudnyk, K. Pasda, M. Brandl, and A. Maier. 2022. "Investigations at the Epigravettian Site of Barmaky in Volhynia, North-West Ukraine: Analyses and Taxonomic Reflections." *Quartär–Internationales Jahrbuch zur Erforschung des Eiszeitalters und der Steinzeit* 69: 105–144.

Chazan, M. 2017. "Toward a Long Prehistory of Fire." *Current Anthropology* 58, no. S16: S351–S359.

Chernysh, A. P. 1977. "Multilayered Paleolithic Site Korman IV and Its Place in the Paleolithic." In *The Multilayer Paleolithic Site Korman IV on the Middle Dniester*, edited by G. I. Goretski and S. M. Tzeitlin, 7–77. Nauka.

Chernysh, A. P. 1987. "The Standard Multilayered Site Molodova V: Archaelogy." In *The Multilayered Paleolithic Site Molodova V: The Stone Age Men and Environment*, edited by I. K. Ivanova and S. M. Tzeitlin, 7–94. Nauka.

Clark, A. E., S. Ranlett, and M. C. Stiner. 2022. "Domestic Spaces as Crucibles of Paleolithic Culture: An Archaeological Perspective." *Journal of Human Evolution* 172: 103266.

Demay, L., M. A. Julien, M. Anghelinu, et al. 2021. "Study of Human Behaviors During the Late Pleniglacial in the East European Plain Through Their Relation to the Animal World." *Quaternary International* 581: 258–289. https://doi.org/10.1016/j.quaint.2020.10.047.

Demidenko, Y. E. 2021. "South of Eastern Europe and Upper Paleolithic Diversity Around the Last Glacial Maximum." *Quaternary International* 581–582: 290–295. https://doi.org/10.1016/j.quaint.2020.07.002.

Dibble, H. L., A. Abodolahzadeh, V. Aldeias, P. Goldberg, S. P. McPherron, and D. M. Sandgathe. 2017. "How Did Hominins Adapt to Ice Age Europe Without Fire?" *Current Anthropology* 58, no. S16: S278–S287. https://doi.org/10.1086/692628.

Dibble, H. L., D. Sandgathe, P. Goldberg, S. McPherron, and V. Aldeias. 2018. "Were Western European Neandertals Able to Make Fire?" *Journal of Paleolithic Archaeology* 1, no. 1: 54–79. https://doi.org/10.1007/s41982-017-0002-6.

Ellingham, S. T. D., T. J. U. Thompson, M. Islam, and G. Taylor. 2015. "Estimating Temperature Exposure of Burnt Bone—A Methodological Review." *Science & Justice* 55, no. 3: 181–188. https://doi.org/10.1016/j.scijus.2014.12.002.

Fan, Z., J. E. Herrick, R. Saltzman, et al. 2017. "Measurement of Soil Color: A Comparison Between Smartphone Camera and the Munsell Color Charts." *Soil Science Society of America Journal* 81, no. 5: 1139–1146.

Ferro-Vázquez, C., C. Mallol, and V. Aldeias. 2021. "Simply Red? A Systematic Colour-Based Method for Identifying Archaeological Fires." *Geoarchaeology* 37, no. 2: 284–303. https://doi.org/10.1002/gea.21886.

Galanidou, N. 1997. *"Home is Where the Hearth is" the Spatial Organisation of the Upper Paleolithic Rockshelter Occupations at Klithi and Kastritsa in Northwest Greece*. Bar.

Gallo, G., M. Fyhrie, C. Paine, et al. 2021. "Characterization of Structural Changes in Modern and Archaeological Burnt Bone: Implications for Differential Preservation Bias." *PLoS One* 16, no. 7: e0254529. https://doi.org/10.1371/journal.pone.0254529.

Gilligan, I. 2010. "The Prehistoric Development of Clothing: Archaeological Implications of a Thermal Model." *Journal of Archaeological Method and Theory* 17, no. 1: 15–80. https://doi.org/10.1007/s10816-009-9076-x.

Goldberg, P., C. E. Miller, and S. M. Mentzer. 2017. "Recognizing Fire in the Paleolithic Archaeological Record." *Current Anthropology* 58, no. S16: S175–S190. https://doi.org/10.1086/692729.

Gowlett, J. A. J. 2006. "The Early Settlement of Northern Europe: Fire History in the Context of Climate Change and the Social Brain." *Comptes Rendus Palevol* 5, no. 1–2: 299–310. https://doi.org/10.1016/j.crpv.2005.10.008.

Haburaj, V. 2021. "Exploring Spectral Imaging as a Tool for Stratigraphic Analysis." Doctoral diss.

Haburaj, V., J. Krause, S. Pless, B. Waske, and B. Schütt. 2019. "Evaluating the Potential of Semi-Automated Image Analysis for Delimiting Soil and Sediment Layers." *Journal of Field Archaeology* 44, no. 8: 538–549.

Haesaerts, P., I. Borziac, V. Chirica, F. Damblon, and L. Koulakovska. 2007. "Cadre stratigraphique et chronologique du Gravettien en Europe centrale." *Paléo* 19: 31–51.

Haesaerts, P., I. Borziak, V. Chirica, F. Damblon, L. Koulakovska, and J. Van Der Plicht. 2003. "The East Carpathian Loess Record: A Reference for the Middle and Late Pleniglacial Stratigraphy in Central Europe [La séquence loessique du domaine est-carpatique: une référence pour le Pléniglaciaire moyen et supérieur d'Europe centrale.]." *Quaternaire* 14, no. 3: 163–188. https://doi.org/10.3406/quate.2003.1740.

Haesaerts, P., S. Péan, H. Valladas, F. Damblon, and D. Nuzhnyi. 2015. "Contribution à la stratigraphie du site paléolithique de Mezhyrich (Ukraine)." *L'Anthropologie* 119, no. 4: 364–393.

Hauck, T. C., N. Nolde, R. Ruka, I. Gjipali, J. Dreier, and N. Mayer. 2017. "After the Cold: Epigravettian Hunter-Gatherers in Blazi Cave (Albania)." *Quaternary International* 450: 150–163. https://doi.org/10.1016/j.quaint.2016.11.045.

Heil, J., B. Marschner, and B. Stumpe. 2020. "Digital Photography as a Tool for Microscale Mapping of Soil Organic Carbon and Iron Oxides." *Catena* 193: 104610.

Henry, A. G. 2017. "Neanderthal Cooking and the Costs of Fire." *Current Anthropology* 58, no. S16: S329–S336.

Henry, A. G., T. Büdel, and P.-L. Bazin. 2018. "Towards an Understanding of the Costs of Fire." *Quaternary International* 493: 96–105. https://doi.org/10.1016/j.quaint.2018.06.037.

Hoare, S. 2020. "Assessing the Function of Palaeolithic Hearths: Experiments on Intensity of Luminosity and Radiative Heat Outputs from Different Fuel Sources." *Journal of Paleolithic Archaeology* 3: 537–565. https://doi.org/10.1007/s41982-019-00047-z.

Hoffecker, J. F. 2005. "Innovation and Technological Knowledge in the Upper Paleolithic of Northern Eurasia." *Evolutionary Anthropology: Issues, News, and Reviews* 14, no. 5: 186–198. https://doi.org/10.1002/evan.20066.

Hughes, P. D., and P. L. Gibbard. 2015. "A Stratigraphical Basis for the Last Glacial Maximum (LGM)." *Quaternary International* 383: 174–185. https://doi.org/10.1016/j.quaint.2014.06.006.

Karkanas, P. 2021. "All about Wood Ash: Long Term Fire Experiments Reveal Unknown Aspects of the Formation and Preservation of Ash With Critical Implications on the Emergence and Use of Fire in the Past." *Journal of Archaeological Science* 135: 105476. https://doi.org/10.1016/j.jas.2021.105476.

Karkanas, P., J.-P. Rigaud, J. F. Simek, R. M. Albert, and S. Weiner. 2002. "Ash Bones and Guano: A Study of the Minerals and Phytoliths in the Sediments of Grotte XVI, Dordogne, France." *Journal of Archaeological Science* 29, no. 7: 721–732. https://doi.org/10.1006/jasc.2001.0742.

Klein, R. G. 1973. "Ice-Age Hunters of the Ukraine." University of Chicago Press.

Klein, R. G. 1974. "Ice-Age Hunters of the Ukraine." *Scientific American* 230, no. 6: 96–105.

Kulakovska, L., O. Kononenko, P. Haesaerts, et al. 2021. "The New Upper Palaeolithic Site Korman' 9 in the Middle Dniester Valley (Ukraine): Human Occupation During the Last Glacial Maximum." *Quaternary International* 587–588: 230–250. https://doi.org/10.1016/j.quaint.2021.02.021.

Kulakovska, L., V. Usik, P. Haesaerts, B. Ridush, T. Uthmeier, and T. C. Hauck. 2015. "Upper Paleolithic of Middle Dniester: Doroshivtsi III Site." *Quaternary International* 359–360: 347–361. https://doi.org/10.1016/j.quaint.2014.10.034.

Kulakovska, L. V., V. I. Usyk, P. Haesarts, S. Pirson, O. M. Kononenko, and P. Nigst. 2019. "The Upper Paleolithic Site Korman' 9." *Archaeology and Early History of Ukraine* 32: 111–125. https://doi.org/10.37445/adiu.2019.03.09.

Levin, N., E. Ben-Dor, and A. Singer. 2005. "A Digital Camera as a Tool to Measure Colour Indices and Related Properties of Sandy Soils in Semi-Arid Environments." *International Journal of Remote Sensing* 26, no. 24: 5475–5492.

Maier, A., L. Tharandt, F. Linsel, V. Krakov, and P. Ludwig. 2023. "Where the Grass Is Greener—Large-Scale Phenological Patterns and Their Explanatory Potential for the Distribution of Paleolithic Hunter-Gatherers in Europe." *Journal of Archaeological Method and Theory* 31. no. 3: 918–945. https://doi.org/10.1007/s10816-023-09628-3.

Mallol, C., and A. Henry. 2017. "Ethnoarchaeology of Paleolithic Fire: Methodological Considerations." *Current Anthropology* 58, no. S16: S217–S229. https://doi.org/10.1086/691422.

Mallol, C., C. M. Hernández, D. Cabanes, et al. 2013a. "Human Actions Performed on Simple Combustion Structures: An Experimental Approach to the Study of Middle Palaeolithic Fire." *Quaternary International* 315: 3–15. https://doi.org/10.1016/j.quaint.2013.04.009.

Mallol, C., C. M. Hernández, D. Cabanes, et al. 2013b. "The Black Layer of Middle Palaeolithic Combustion Structures. Interpretation and Archaeostratigraphic Implications." *Journal of Archaeological Science* 40, no. 5: 2515–2537. https://doi.org/10.1016/j.jas.2012.09.017.

Mallol, C., F. W. Marlowe, B. M. Wood, and C. C. Porter. 2007. "Earth, Wind, and Fire: Ethnoarchaeological Signals of Hadza Fires." *Journal of Archaeological Science* 34, no. 12: 2035–2052. https://doi.org/10.1016/j.jas.2007.02.002.

Mallol, C., S. M. Mentzer, and C. E. Miller. 2017. "Combustion Features." In *Archaeological Soil and Sediment Micromorphology*, edited by C. Nicosia and G. Stoops, 299–330. https://doi.org/10.1002/9781118941065.ch31.

March, R. J., A. Lucquin, D. Joly, J. C. Ferreri, and M. Muhieddine. 2014. "Processes of Formation and Alteration of Archaeological Fire Structures: Complexity Viewed in the Light of Experimental Approaches." *Journal of Archaeological Method and Theory* 21: 1–45.

Marquer, L., V. Lebreton, T. Otto, and E. Messager. 2015. "Étude des macro-, méso- et micro-charbons du site épigravettien de Mezhyrich (Ukraine): données taphonomiques et anthracologiques." *L'Anthropologie* 119, no. 4: 487–504. https://doi.org/10.1016/j.anthro.2015.07.006.

Marquer, L., V. Lebreton, T. Otto, et al. 2012. "Charcoal Scarcity in Epigravettian Settlements With Mammoth Bone Dwellings: The Taphonomic Evidence From Mezhyrich (Ukraine)." *Journal of Archaeological Science* 39, no. 1: 109–120. https://doi.org/10.1016/j.jas.2011.09.008.

Matthiesen, H., J. B. Jensen, D. Gregory, J. Hollesen, and B. Elberling. 2013. "Degradation of Archaeological Wood Under Freezing and Thawing Conditions—Effects of Permafrost and Climate Change." *Archaeometry* 56, no. 3: 479–495. https://doi.org/10.1111/arcm.12023.

McCauley, B., M. Collard, and D. Sandgathe. 2020. "A Cross-Cultural Survey of On-Site Fire Use by Recent Hunter-Gatherers: Implications for Research on Palaeolithic Pyrotechnology." *Journal of Paleolithic Archaeology* 3: 566–584. https://doi.org/10.1007/s41982-020-00052-7.

Mentzer, S. M. 2014. "Microarchaeological Approaches to the Identification and Interpretation of Combustion Features in Prehistoric Archaeological Sites." *Journal of Archaeological Method and Theory* 21, no. 3: 616–668. https://doi.org/10.1007/s10816-012-9163-2.

Miller, C. E., N. J. Conard, P. Goldberg, and F. Berna. 2010. "Dumping, Sweeping and Trampling: Experimental Micromorphological Analysis of Anthropogenically Modified Combustion Features." *Palethnologie: Archéologie et Sciences Humaines* 2.

Mix, A. 2001. "Environmental Processes of the Ice Age: Land, Oceans, Glaciers (EPILOG)." *Quaternary Science Reviews* 20, no. 4: 627–657. https://doi.org/10.1016/s0277-3791(00)00145-1.

Moreau, L., C. Draily, J.-M. Cordy, et al. 2021. "Adaptive Trade-Offs Towards the Last Glacial Maximum in North-Western Europe: A Multidisciplinary View From Walou Cave." *Journal of Paleolithic Archaeology* 4, no. 2: 11. https://doi.org/10.1007/s41982-021-00078-5.

Murphree, W. C., and V. Aldeias. 2022. "The Evolution of Pyrotechnology in the Upper Palaeolithic of Europe." *Archaeological and Anthropological Sciences* 14, no. 10: 202. https://doi.org/10.1007/s12520-022-01660-w.

Nigst, P. R., T. Libois, P. Haesaerts, et al. 2021. "The Mid Upper Palaeolithic (Gravettian) Sequence of Mitoc-Malu Galben (Romania): New Fieldwork Between 2013 and 2016-Preliminary Results and Perspectives." *Quaternary International* 587: 189–209.

Noiret, P. 2004. "Le Paléolithique supérieur de la Moldavie." *L'Anthropologie* 108, no. 3–4: 425–470. https://doi.org/10.1016/j.anthro.2004.10.003.

Noiret, P. 2009. "Le Paléolithique supérieur de la Moldavie. Essai de synthèse d'une évolution multi-culturelle." *Études et Recherches archéologiques de l'Université de Liège* 121: 31351449.

Noiret, P., T. Libois, V. Chirica, et al. 2021. "40 Years of Excavations at Mitoc–Malu Galben (Romania): Changing Fieldwork Methodologies and Implications for the Comparability of Archaeological Assemblages." *L'Anthropologie* 125, no. 4: 102919. https://doi.org/10.1016/j.anthro.2021.102919.

Noiret, P., and M. Otte. 2010. "Aurignacian and Gravettian Occupations in Eastern Europe Between 33,000 and 23,000 Uncal BP." In *OIS 3 Conference*. https://api.semanticscholar.org/CorpusID:54742370.

Nuzhnyi, D. 2006. "The Latest Epigravettian Assemblages of the Middle Dnieper Basin (Northern Ukraine)." *Archaeologia Baltica* 7: 58–93.

O'Donnell, T. K., K. W. Goyne, R. J. Miles, C. Baffaut, S. H. Anderson, and K. A. Sudduth. 2011. "Determination of Representative Elementary Areas for Soil Redoximorphic Features Identified by Digital Image Processing." *Geoderma* 161, no. 3–4: 138–146.

Pryor, A. J. E., A. Pullen, D. G. Beresford-Jones, J. A. Svoboda, and C. S. Gamble. 2016. "Reflections on Gravettian Firewood Procurement Near the Pavlov Hills, Czech Republic." *Journal of Anthropological Archaeology* 43: 1–12. https://doi.org/10.1016/j.jaa.2016.05.003.

Roebroeks, W., and P. Villa. 2011. "On the Earliest Evidence for Habitual Use of Fire in Europe." In *Proceedings of the National Academy of Sciences of the United States of America* 108, no. 13: 5209–5214. https://doi.org/10.1073/pnas.1018116108.

Rolland, N. 2004. "Was the Emergence of Home Bases and Domestic Fire a Punctuated Event? A Review of the Middle Pleistocene Record in Eurasia." *Asian Perspectives* 43, no. 2: 248–280. https://doi.org/10.1353/asi.2004.0027.

Rolland, N. 2018. "Homebases in Paleolithic Archaeology." In *The International Encyclopedia of Anthropology*, edited by H. Callan, 1–7. https://doi.org/10.1002/9781118924396.wbiea1784.

Sandgathe, D. M. 2017. "Identifying and Describing Pattern and Process in the Evolution of Hominin Use of Fire." *Current Anthropology* 58, no. S16: S360–S370. https://doi.org/10.1086/691459.

Sandgathe, D. M., H. L. Dibble, P. Goldberg, et al. 2011. "Timing of the Appearance of Habitual Fire Use." *Proceedings of the National Academy of Sciences of the United States of America* 108, no. 29: E298. https://doi.org/10.1073/pnas.1106759108.

Schiegl, S., P. Goldberg, H.-U. Pfretzschner, and N. J. Conard. 2003. "Paleolithic Burnt Bone Horizons From the Swabian Jura: Distinguishing Betweenin Situ Fireplaces and Dumping Areas." *Geoarchaeology* 18, no. 5: 541–565. https://doi.org/10.1002/gea.10080.

Schilt, F., A. Verpoorte, and W. Antl. 2017. "Micromorphology of an Upper Paleolithic Cultural Layer at Grub-Kranawetberg, Austria." *Journal of Archaeological Science: Reports* 14: 152–162. https://doi.org/10.1016/j.jasrep.2017.05.041.

Soffer, O., J. M. Adovasio, N. L. Kornietz, et al. 1997. "Cultural Stratigraphy at Mezhirich, an Upper Palaeolithic Site in Ukraine With Multiple Occupations." *Antiquity* 71, no. 271: 48–62.

Sorensen, A., W. Roebroeks, and A. van Gijn. 2014. "Fire Production in the Deep Past? The Expedient Strike—A Light Model." *Journal of Archaeological Science* 42: 476–486. https://doi.org/10.1016/j.jas.2013.11.032.

Sorensen, A. C. 2017. "On the Relationship Between Climate and Neandertal Fire Use During the Last Glacial in South-West France." *Quaternary International* 436: 114–128. https://doi.org/10.1016/j.quaint.2016.10.003.

Speth, J. D. 2017. "Putrid Meat and Fish in the Eurasian Middle and Upper Paleolithic: Are We Missing a Key Part of Neanderthal and Modern Human Diet?" *PaleoAnthropology* 2017: 44–72.

Stahlschmidt, M. C., C. Mallol, and C. E. Miller. 2020. "Fire as an Artifact—Advances in Paleolithic Combustion Structure Studies: Introduction to the Special Issue." *Journal of Paleolithic Archaeology* 3, no. 4: 503–508. https://doi.org/10.1007/s41982-020-00074-1.

Stahlschmidt, M. C., C. E. Miller, B. Ligouis, et al. 2015. "On the Evidence for Human Use and Control of Fire at Schöningen." *Journal of Human Evolution* 89: 181–201.

Stapert, D. 1989. "The Ring and Sector Method: Intrasite Spatial Analysis of Stone Age Sites, With Special Reference to Pincevent." *Palaeohistoria* 31: 1–57.

Stiner, M. C., V. Dimitrijević, D. Mihailović, and S. L. Kuhn. 2022. "Velika Pećina: Zooarchaeology, Taphonomy and Technology of a LGM Upper Paleolithic Site in the Central Balkans (Serbia)." *Journal of Archaeological Science: Reports* 41: 103328. https://doi.org/10.1016/j.jasrep.2021.103328.

Stiner, M. C., S. L. Kuhn, S. Weiner, and O. Bar-Yosef. 1995. "Differential Burning, Recrystallization, and Fragmentation of Archaeological Bone." *Journal of Archaeological Science* 22, no. 2: 223–237. https://doi.org/10.1006/jasc.1995.0024.

Stoops, G. 2003. *Guidelines for Analysis and Description of Soil and Regolith Thin Sections*. Soil Science Society of America Inc.

Straus, L. G. 2015. "The Human Occupation of Southwestern Europe During the Last Glacial Maximum." *Journal of Anthropological Research* 71, no. 4: 465–492. https://doi.org/10.3998/jar.0521004.0071.401.

Svoboda, J., M. Novák, S. Sázelová, Š. Hladilová, and P. Škrdla. 2018. "Dolní Věstonice I. Excavations 1990–1993." *Přehled výzkumůs* 59, no. 1: 27–60.

Škrdla, P., M. Vlach, L. Nejman, J. Bartík, Y. E. Demidenko, and T. Rychtaříková. 2021. "Settlement Strategies in Eastern Central Europe during the Maximum Extent of the Last Glacial Ice Sheet." *Quaternary International* 581–582: 164–174. https://doi.org/10.1016/j.quaint.2020.09.047.

Théry-Parisot, I. 2002. "Fuel Management (Bone and Wood) During the Lower Aurignacian in the Pataud Rock Shelter (Lower Palaeolithic, Les Eyzies de Tayac, Dordogne, France). Contribution of Experimentation." *Journal of Archaeological Science* 29, no. 12: 1415–1421. https://doi.org/10.1006/jasc.2001.0781.

Théry-Parisot, I., S. Costamagno, J.-P. Brugal, P. Fosse, and R. Guilbert. 2005. *The Use of Bone as Fuel During the Palaeolithic, Experimental Study of Bone Combustible Properties*. Oxbow Books.

Viscarra Rossel, R. A., Y. Fouad, and C. Walter. 2008. "Using a Digital Camera to Measure Soil Organic Carbon and Iron Contents." *Biosystems Engineering* 100, no. 2: 149–159.

Van Vliet-Lanoë, B. 1985. "Frost Effects in Soils." *Soils and Quaternary Landscape Evolution* 117: 158.

Van Vliet-Lanoë, B. 2010. "Frost Action." In *Interpretation of Micromorphological Features of Soils and Regoliths*, edited by G. Stoops, V. Marcelino and F. Mees, 81–108. Elsevier.

Willis, K., and T. Van Andel. 2004. "Trees or no Trees? The Environments of Central and Eastern Europe During the Last Glaciation." *Quaternary Science Reviews* 23, no. 23–24: 2369–2387. https://doi.org/10.1016/j.quascirev.2004.06.002.

Wrangham, R. 2017. "Control of Fire in the Paleolithic: Evaluating the Cooking Hypothesis." *Current Anthropology* 58, no. S16: S303–S313.

Supporting Information

Additional supporting information can be found online in the Supporting Information section.